Global and Planetary Change 199 (2021) 103428

Contents lists available at ScienceDirect

Global and Planetary Change

journal homepage: www.elsevier.com/locate/gloplacha

End-Triassic crisis and "unreefing" led to the demise of the Dachstein carbonate platform: A revised model and evidence from the Transdanubian Range, Hungary

József Pálfy [a,b,*], Zsófia Kovács [a,c,d,e], Attila Demény [f], Zsolt Vallner [a,c]

[a] Department of Geology, Eötvös Loránd University, Budapest H-1117, Hungary
[b] MTA–MTM–ELTE Research Group for Paleontology, POB 137, Budapest H-1431, Hungary
[c] Isotope Climatology and Environmental Research Centre (ICER), Institute for Nuclear Research, Bem square 18/C, Debrecen H-4026, Hungary
[d] Institute for Earth Sciences (Geology and Paleontology), University of Graz, Heinrichstrasse 26, Graz 8010, Austria
[e] Department of Geology, University of Lund, Sölvegatan 12, Lund 22362, Sweden
[f] Research Centre for Astronomy and Earth Sciences, Institute for Geological and Geochemical Research, Budaörsi út 45, Budapest H-1112, Hungary

ARTICLE INFO

Keywords:
Triassic-Jurassic boundary
Carbon isotope
Platform drowning
Submarine erosion
Ecosystem collapse
Astrochronology

ABSTRACT

The Dachstein platform was an extensive carbonate platform developed on the westernmost shelf of the Neotethys during the Late Triassic, now preserved in various tectonic units disrupted during the Alpine orogeny. Despite being the focus of a multitude of sedimentological, paleontological and other studies, the demise of this platform remains controversial, with contrasting views on the timing and causes of cessation of its growth, the duration of the gap above, which at many places includes the Triassic-Jurassic boundary (TJB), and the depositional environment of overlying strata.

Here we present new carbonate sedimentological, stable isotope and cyclostratigraphic data from sections in the Transdanubian Range (Hungary) which capture the termination of uppermost Triassic Dachstein Limestone and the onset of Hettangian (Early Jurassic) sedimentation following a hiatus. Previously, the TJB in the Transdanubian Range was regarded as a textbook case of a tectonically-driven platform drowning event or, alternatively, cessation of carbonate production due to emergence caused by a significant sea level fall at the TJB. However, recognition of global biotic change and environmental perturbations at the TJB calls for an assessment of their possible role in the demise of the Dachstein platform.

Oxygen and carbon isotopic composition of bulk carbonates were measured in sections at Kőris-hegy (Bakony Mts.), Tata (Tata Horst), and Vöröshíd (Gerecse Mts.) Paleogeographically, these three sections represent a proximal to distal platform transect. Other sections at Pisznice and Tölgyhát (Gerecse Mts.) yielded additional sedimentological data. The sharp surface separating the Dachstein Limestone from the overlying Jurassic formations carries no or only minimal relief at outcrop scale. Thin section studies reveal small-scale irregularities, stylolites, microborings with ferruginous filling, or a thin clay-rich layer at the TJB, indicative of a submarine, or perhaps polygenetic, hardground. In the first meters of the lowermost Jurassic beds abundant ooids occur, and crinoids become common. In each of the studied sections, an abrupt negative carbon isotope shift is recorded at the TJB, and a gradual rebound to more positive values characterizes the lowermost Jurassic strata. Chemostratigraphy allows correlation with sections elsewhere. In the Transdanubian Range, the initial carbon isotope excursion and at least the first part of the purported main carbon isotope excursion are not preserved due to the gap at the TJB. Combined bio- and cyclostratigraphy of lowermost Jurassic strata permits an astrochronologic duration estimate of the early Hettangian hiatus that was not longer than a few hundreds of thousand years.

Our results highlight the role of submarine erosion, perhaps partly related to acidification, and point to an abrupt change in carbonate production related to the end-Triassic extinction of several groups in the platform system. "Unreefing", the ecological collapse of reefs, led to a regime shift, the transformation of the rimmed platform to a carbonate ramp, with a significant gap in production and preservation of carbonate sediment. This model is not uniformly applicable to Late Triassic platforms as several of them, unlike the Dachstein platform,

* Corresponding author at: Department of Geology, Eötvös Loránd University, Budapest H-1117, Hungary
E-mail address: palfy@elte.hu (J. Pálfy).

https://doi.org/10.1016/j.gloplacha.2021.103428
Received 30 April 2020; Received in revised form 9 January 2021; Accepted 13 January 2021
Available online 20 January 2021

survived with unrimmed architecture in the Early Jurassic elsewhere on the Neotethyan shelf. However, the model may explain features of the carbonate platform sedimentary record across other events with reef collapse.

1. Introduction

The Dachstein carbonate platform is one of the most extensive and best studied Phanerozoic carbonate platforms that developed on the westernmost Neotethyan shelf during the Late Triassic. The Dachstein platform occupied parts of a broad, up to 300 km-wide shelf belt on the European passive margin (Krystyn et al. 2005) where an up to 2 km-thick succession of alternating well-bedded to massive and stromatolitic dolomite, the Main Dolomite (Hauptdolomit) Formation and the overlying (and partly laterally adjacent) limestone with prominent cyclicity, the Dachstein Formation was deposited from late Carnian to Rhaetian time. The Dachstein platform was dismembered during the Alpine orogeny but its originally contiguous parts are now preserved in the Austroalpine Units in the classical type area of the Northern Calcareous Alps and also in the Transdanubian Range in Hungary (Haas et al. 1995). Although these shallow marine carbonates have been in the focus of many classical and modern studies, some important issues remain debated. Cyclic stratal patterns in the Dachstein Formation were described as Lofer cycles composed of members A, B, and C that were formed in supra-, inter-, and subtidal depositional environments, respectively, and interpreted to reflect orbitally controlled sea-level changes in peritidal deposits (Fischer 1964; Haas, 1994; Enos and Samankassou 1998; Haas et al. 2007). Lagoons of the inner Dachstein platform in the Northern Calcareous Alps were fringed by prolific reefs that harbored a rich biota (Bernecker 2005; Martindale et al. 2013): the Dachstein reefs faced the open oceanic Hallstatt Basin whereas on the opposing side the Rhaetian *Oberrhätkalk* reefs bordered intraplatform basins such as the Eiberg Basin (Mandl 2000). However, the timing and causes of demise of the Dachstein platform system remain controversial. Although locally the shallow marine limestone is overlain by middle Rhaetian basinal deposits (Krystyn et al. 2009), elsewhere deposition of the Dachstein Formation continued until the end of the Rhaetian (Missoni and Gawlick 2011). Termination of shallow marine platform sedimentation is most commonly interpreted as a drowning event related to the onset of extensional tectonics (Mandl 2000), but cessation of growth of a reef complex at Steinplatte was also ascribed to rapid sea level fall of an estimated 150 m (Krystyn et al. 2005). Only a few authors speculated that the ecological consequences of the end-Triassic mass extinction may have also played a significant role (Gawlick et al. 1999, 2009).

In the Transdanubian Range, the Main Dolomite and Dachstein Limestone are the areally and volumetrically most extensive formations. Termination of platform growth, and the unconformity at the top of the Dachstein Formation have long been regarded to mark the Triassic-Jurassic boundary (TJB), as overlying Jurassic strata are lithologically different and a hiatus of variable duration is present across the entire Transdanubian Range. Stratigraphic studies in the Bakony Mts., Tata Horst and Gerecse Mts. led to different interpretations about the demise of the Late Triassic Dachstein platform, either due to emergence or drowning, both potentially ascribed to either eustatic sea level change or synsedimentary tectonic forcing (Fig. 1). Emergence and subaerial exposure were suggested in studies of TJB sections both in the Gerecse (Vigh 1936, 1961a, 1961b) and Bakony Mts. (Császár and Oravecz-Scheffer 1987). On the contrary Haas (1995a, 1995b), inferred platform drowning both in the Bakony and Gerecse Mts., where subsidence was explained by incipient rifting of the Ligurian-Penninic oceanic branch and related regional extension in the Transdanubian Range (Vörös and Galácz 1998). Here basin-scale differential subsidence dominated from the Early Jurassic but tilted blocks along listric normal faults may have led to temporary emergence of parts of the platform. A detailed study of the Tata Horst led to a tentative suggestion of

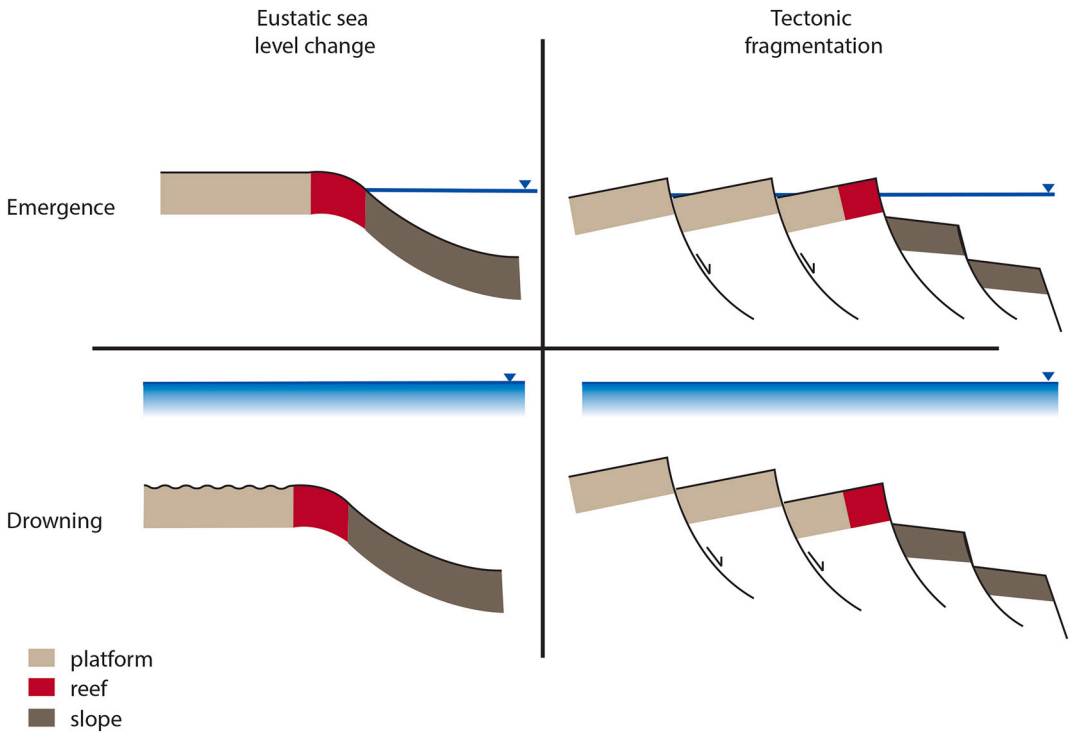

Fig. 1. Contrasting models proposed previously to explain the demise of the Dachstein platform in the Transdanubian Range. Emergence by sea level fall was proposed by Vigh (1933, 1961) (see upper left), possibly in combination with tectonic fragmentation (Győri 2014) (upper right). Drowning with a role of submarine dissolution and erosion suggested by Fülöp (1976) (lower left), tectonic subsidence emphasized by Haas et al. (1995) (lower right).

submarine dissolution as an alternative explanation of the TJB surface on top of the Dachstein Fm (Fülöp 1976).

Recently, a multitude of studies emphasized the significance of the end-Triassic extinction and concomitant environmental changes for the entire Earth system, as reviewed by Pálfy and Kocsis (2014). Notably, runaway greenhouse warming (McElwain et al. 1999), perturbation of the carbon cycle (Pálfy et al. 2001; Ward et al. 2001; Hesselbo et al. 2002), ocean acidification (Hautmann 2004; Greene et al. 2012), and a major crisis of reef ecosystems (Kiessling et al. 2007) represent potential factors affecting the health and growth of a carbonate platform, which has not yet been fully explored in connection with the fate of the Dachstein platform (Haas et al. 2018).

Here we present the results of a multifaceted study of TJB sections from the Transdanubian Range (Hungary) which record the disconformity that marks the top of the Dachstein Limestone. Sections in our study areas in the Transdanubian Range are closely correlative to the type area of the formation in the Northern Calcareous Alps in Austria. Whereas previous studies emphasized the role of either tectonically-driven drowning and disintegration of the platform, or emergence due to sea level drop at the TJB, the role of other environmental and ecological changes related to the end-Triassic extinction has received much less attention. Our aim is to generate new stratigraphic data from multiple sections in the Transdanubian Range, through combined application of carbonate sedimentology and stable isotope chemostratigraphy, while also obtaining additional constraints from bio- and cyclostratigraphy. The new results are then interpreted in the context of possible causes and processes of the demise of Dachstein platform and the resumption of sedimentation during the earliest Jurassic biotic recovery. We demonstrate that environmental and biotic changes were fundamental drivers, more important than previously recognized.

2. Geological setting

The lower Mesozoic succession of the Transdanubian Range was deposited at the passive margin of the Neotethys and later the newly opening Alpine Tethys, thus its basin evolution was controlled by tectonic processes related to the opening of the Neotethys and Ligurian-Penninic oceanic branches (Haas et al. 1995). Early phase of rifting in the Middle Triassic was followed by filling up the basin during the Carnian, leading to the development of a large platform system. The Main Dolomite (*Hauptdolomit* or *Dolomia Principale* in German and Italian literature, respectively) and the overlying Dachstein Limestone together represent an extensive, tropical shallow carbonate platform system with a combined thickness in excess of 2 km in the Transdanubian Range (Fig. 2) (Haas 2004). Other parts of the once contiguous platform system, disrupted by later phases of tectonic evolution related to the Alpine orogeny, are preserved in the Upper Austroalpine nappe system of the Northern Calcareous Alps, with more distant analogues in the Southern Alps (Haas et al. 1995).

The Jurassic succession of the Transdanubian Range, in sharp contrast to the Upper Triassic, is much less thick, ~500 m in the Zala Basin southwest of the Bakony but thinning significantly to the east in the Gerecse (Vörös and Galácz 1998). Facies variability in the Bakony and Gerecse is expressed in contrasting types of successions, continuous sections and those with gaps, especially after marked differentiation of basin floor topography starting in the Sinemurian. In the Bakony, the Dachstein Limestone is paraconformably overlain by ooidal-oncoidal limestone of the Kardosrét Formation, an up to 200 m thick shallow marine deposit, that distinctly lacks Lofer cyclicity (i.e. facies stacking of subtidal, peritidal and supratidal origin) (Haas 1995a). This unit is pinching out to the northwest, and in Tata and the Gerecse the lowermost Jurassic Pisznice Limestone rests upon the disconformity surface at the top of Dachstein Fm. Ammonites and brachiopods suggest that at Tata and some localities in the Gerecse the basal, massively bedded part of this formation could be at least as old as middle Hettangian (Dulai 1998; Pálfy et al. 2007). Upsection, Sinemurian and Pliensbachian strata

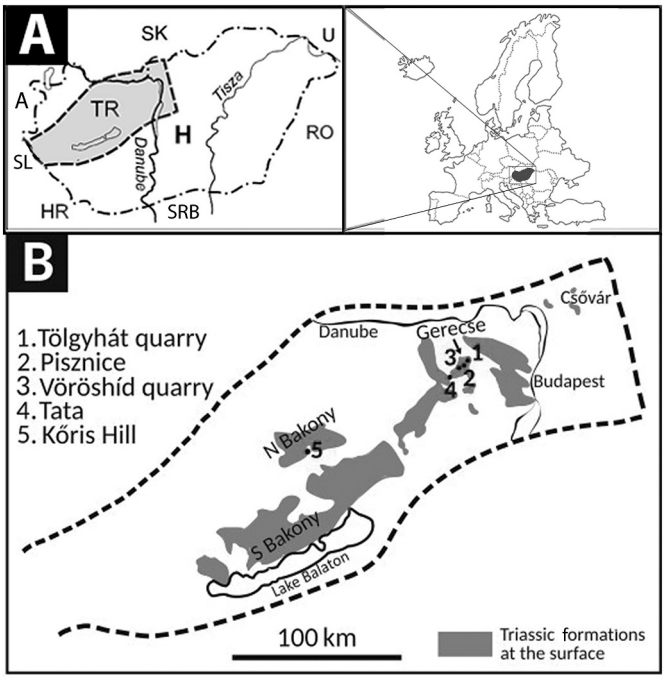

Fig. 2. Location map of the study area in the Transdanubian Range. (A) Index map showing the Transdanubian Range (TR) tectonic unit within Hungary (H) and its geographic context within Europe. (SK: Slovakia, U: Ukraine, RO: Romania, SRB: Serbia, HR: Croatia, SL: Slovenia, A: Austria.) (B) Location of the studied sections and areal extent (grey-shaded areas) of surface exposure of Upper Triassic platform carbonates (after Haas 2002).

in this formation record a transition from neritic to increasingly pelagic depositional environment (Budai et al., 2018). The Schnöll Fm. (formerly included in the Adnet Fm.) represents the closest analogue in the Upper Austroalpine units in the Northern Calcareous Alps (Császár et al. 1998; Haas et al. 2011).

Paleogeographic reconstruction of the Hauptdolomit/Dachstein carbonate platform and overlying lowermost Jurassic deposits is confounded by its dismemberment into thrust sheets that form the nappe stack of the Austroalpine Units exposed in the Northern Calcareous Alps (Gawlick et al. 2009). Although truncated by the Balaton line and the Mid-Hungarian shear zone in the south and concealed under the Neogene cover in the Danube basin in the north, the allochthonous Transdanubian Range is thought to represent the uppermost unit within the Austroalpine nappe stack formed in the Cretaceous (Tari and Horváth 2010). Parts of the Dachstein platform as preserved in the Northern Calcareous Alps and in the Transdanubian Range are now disjunct parts of the Alcapa terrane (Csontos and Vörös 2004), separated by major Cenozoic lateral extrusion (Ratschbacher et al. 1991). However, data from both areas are equally important for understanding the evolution and demise of this platform system. Paleogeographic reconstructions suggest that the Late Triassic position of the Transdanubian Range was intermediate between the Upper Austroalpine units of the Northern Calcareous Alps and the Southern Alps (Haas et al. 1995; Mandl 2000), and alignment of facies belts should take into account a Cenozoic counterclockwise rotation of up to 75–90° (Márton and Márton 1981; Márton and Fodor 2003).

3. Stratigraphy and the TJB in the studied sections

3.1. Gerecse

3.1.1. Tölgyhát

The Tölgyhát quarry represents the most complete and thickest Jurassic succession in the Gerecse, briefly described by Konda (1988). In

this abandoned quarry on the north slope of Gerecse (Fig. 2, 47°43′22.11" N, 18°30′44.76″ E), the lowermost 3 m exposes the topmost layers of Dachstein Fm., here mainly consisting of light grey, thick-bedded limestone with calcite specks (i.e. recrystallized tests of the foraminifer *Triasina hantkeni*). The uppermost one-cm-thick purple layer with fenestral pores is member B of a Lofer cyclothem in the of the Dachstein Fm., overlying a similarly thin layer of clayey limestone (Fig. 3D) that in turn rests upon an irregularly eroded top surface of member A with cm-scale relief. The boundary between the Dachstein Fm. and the paraconformably overlying poorly bedded, massive Pisznice Fm. is sharp and planar (Fig. 3D). Macrofauna in the lowermost Jurassic beds of Pisznice Fm. consists of brachiopods, Dulai (1998) reported the occurrence of 9 species from the basal 3.5 m.

3.1.2. Nagy-Pisznice

Near the SW corner of a large abandoned quarry on Nagy-Pisznice Hill, a natural outcrop (47°41′56.90" N, 18°29′24″ E) exposes c. 3 m of strata across the TJB (Fig. 3A). The topmost, 70-cm-thick bed of Dachstein Fm. comprises grey, micritic limestone that represents member C of a Lofer cyclothem. The lowermost, c. 20-cm-thick, crinoid-bearing light pink limestone beds of the overlying Pisznice Fm. contain rare brachiopods. Some 0.5 m above the TJB the beds become darker, more crinoid-rich and contain intraclasts, with increasingly stylolitic bedding planes. The formation boundary, hence the TJB, is a sharp and slightly irregular, pockmarked surface (Fig. 3A, B). The shallow depressions are commonly filled with ferruginous material or green clay, the latter also occurs as coating, void fills or clasts in the basal Jurassic layer (Fig. 3C). The Nagy-Pisznice quarry section was briefly described by Konda (1985).

3.1.3. Vöröshíd

The abandoned Vöröshíd quarry (47°41′28.38" N, 18°27′47.90″ E) exposes c. 30 m of the Dachstein Fm. and the overlying Pisznice Fm. (Figs. 4A, S1), providing the best exposure of the TJB in the Gerecse Mts. The Dachstein Fm. comprises well-developed Lofer cyclothems, dominated by thick layers of member C, including the topmost Triassic bed that contains abundant foraminifers (*Triasina hantkeni*) and large-sized (10–15 cm) molds of megalodontid bivalves. Some of these molds and additional irregular shaped voids are filled with pink, at some places laminated micritic or crinoidal limestone, genetically related to the overlying Jurassic limestone. The molds and void fills are commonly surrounded by isopachous radiaxial calcite cement of up to 4 mm in width.

Above a 5-cm-thick basal layer, the lower 8 m of the overlying Pisznice Fm. is light pink, thick-bedded, and slightly crinoidal. As in the Dachstein Fm., the lowermost Pisznice Fm. also contains irregular shaped, commonly horizontally elongated voids, with or without an isopachous cement envelope (Fig. 4B). The lowermost 1 m in the Jurassic contains abundant coated grains, whereas higher up crinoid bioclasts become more common, often enriched in pockets with diffuse boundary. Upsection, the next 7 m consists of more thinly-bedded and darker brownish-red limestone.

The contact between the two formations at the TJB is sharp, at some places perfectly planar (Fig. 4B, C), elsewhere with stylolites of 0.5 cm amplitude (Fig. 4D). Truncated molds of large-sized megalodontid bivalves are a spectacular feature of this locality (Lantos 1997). The lower, thick-bedded part yielded a brachiopod fauna of 10 species (Dulai 1998); rare ammonoids also occur 100–130 cm above the TJB but could not be extracted. The oldest identifiable ammonites were found higher, in the thin-bedded member, and indicate Early Sinemurian age (Dulai 1998). The Vöröshíd quarry section was briefly described by Konda (1987). The inferred basin margin depositional environment of Sinemurian strata reflects the evolution of dissected paleotopography after termination of uniform Late Triassic Dachstein platform (Lantos 1997).

3.2. Tata (Kálvária-domb)

In the abandoned quarry yard (47°38′21.56" N, 18°18′54.04″ E)

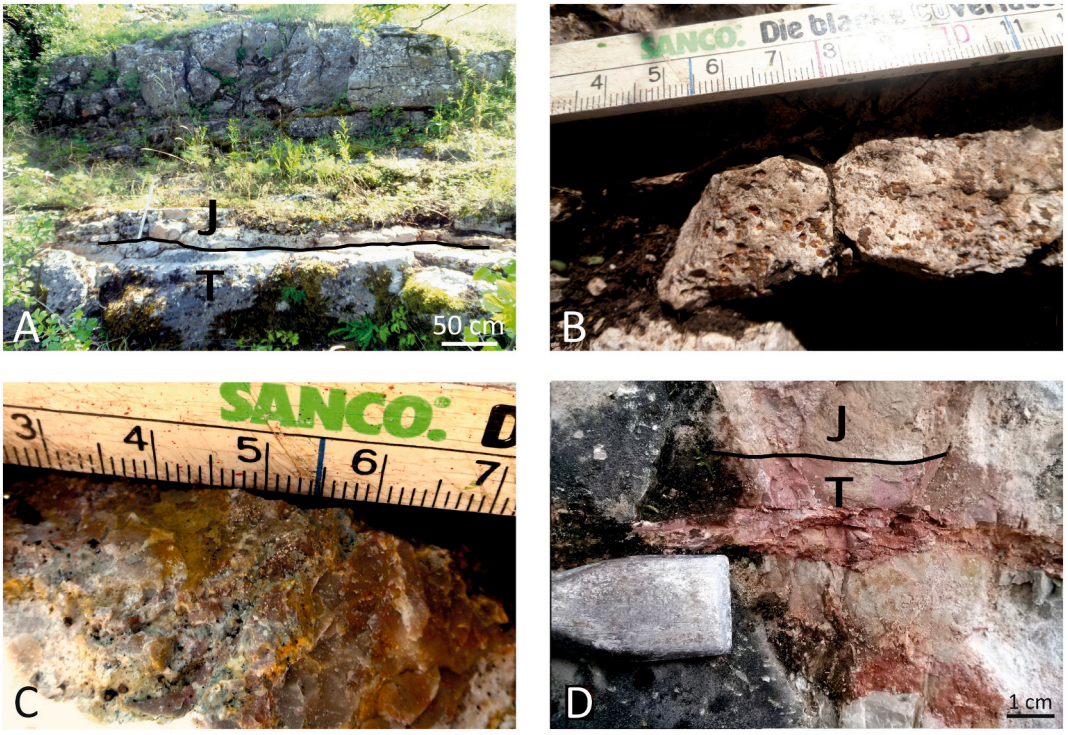

Fig. 3. The TJB in the Pisznice (A–C) and Tölgyhát (D) sections. (A) View of sharp, undulating TJB surface in the Pisznice section. (B) Rounded borings of few mm in diameter with ferruginous filling on the top surface of Dachstein Fm. (Scale in cm.) (C) Thin, green clay film at the TJB surface. (Scale in cm.) (D) Sharp, planar TJB surface above member B in the topmost bed of Dachstein Fm. (For interpretation of the references to color in this figure legend, the reader is referred to the web version of this article.)

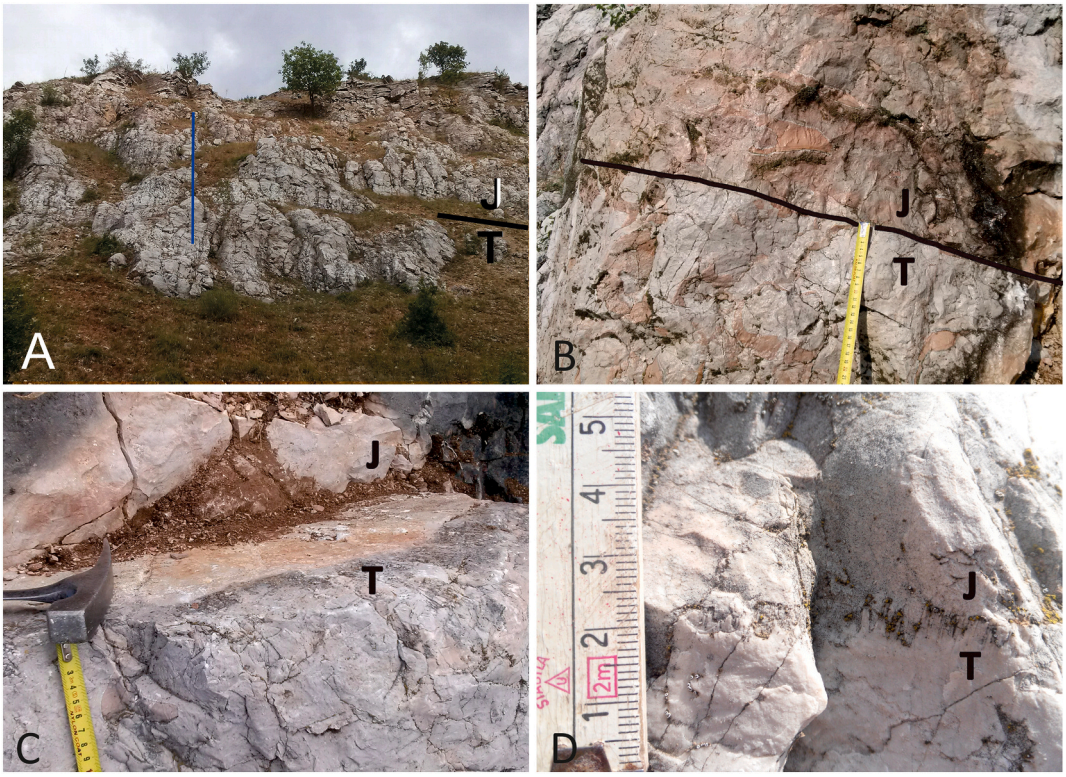

Fig. 4. The TJB in the Vöröshíd quarry section. (A) View of the quarry wall showing the position of TJB and location of the 19.5 m thick profile sampled for stable isotope analyses. (B) Cavities of irregular shape occurring both in the Dachstein and Pisznice Fm., filled by red micrite, in some cases surrounded by isopachous white calcite cement. (C) Planar TJB surface. (D) Stylolytes with amplitude of 0.5 cm at the TJB. (For interpretation of the references to color in this figure legend, the reader is referred to the web version of this article.)

beneath the Calvary statues outside the Geological Garden in Tata (Haas and Hámor 2001), the uppermost part of Dachstein Fm. and lowermost part of Pisznice Fm. are exposed in a combined thickness of 18 m (Fig. 5C). Members C and B dominate the Lofer cyclothems in the uppermost Triassic. Thick beds of member C contain several types of voids, including molds after large megalodontid bivalves and cavities of irregular shape, both are commonly filled with red micrite within a white fibrous calcite envelope (Győri 2014) (Fig. 5A). Members B occur as 10–25 cm thick laminated layers of microbial mat origin. Rare black pebbles and traces of paleosol indicate the presence of member A. A network of neptunian dykes with red Jurassic micritic limestone fill crosscuts the uppermost part of the Dachstein Fm. (Fig. 5D).

The contact between the two formations is near perfectly planar. Laterally, not along the sampled profile but elsewhere within the Geological Garden, the topmost bedding plane of the Dachstein Fm. is exposed extensively. Its surface is densely covered with shallow, rounded, unfilled depressions of 0.5–2.5 mm diameter (Fig. 5B), the adjacent ones are commonly merged. In the basal part of the overlying massive to thick-bedded pink limestone of the Pisznice Fm., an interval 50 to 90 cm above the TJB contains abundant coated grains and some coated macrofossils. The Mesozoic section of the Tata horst has a long history of study (Koch 1909; Szabó 1961) culminating in the monograph of Fülöp (1976), who surmised on the significance of the TJB surface and first suggested the possibility of submarine erosion. Later studies also considered the complexity of the issue but observed some 1.5 m difference at outcrop-scale in the truncated top of the Dachstein Fm. and argued for emergence and subaerial erosion (Haas et al. 2018).

In the first biostratigraphic study at Tata (Koch 1909) the TJB was recognized after assigning a Rhaetian age for the Dachstein Limestone based on its megalodontid bivalve fauna and a middle or upper Hettangian age for the basal Jurassic on the basis of ammonoid finds, also noting the common brachiopods. Szabó (1961) identified further ammonoid taxa and agreed with a mid-Hettangian age assignment (Megastoma Zone as defined in the Alps) for the oldest Jurassic strata, explaining the hiatus above the Dachstein Limestone with tectonic activity. Within the monographic treatment of the geology of Tata (Fülöp 1976), Géczy re-studied the lowermost Jurassic ammonoids and found no firm evidence for Jurassic older than the Upper Hettangian Marmorea Zone. A more recent study suggested the presence of *Alsatites*, *Discamphiceras*, and *Paracaloceras*, on the basis of distinctive cross sections of inextractable specimens in an oncoidal layer 30–70 cm above the TJB (Pálfy et al. 2007). This assemblage may hint at the presence of the mid to late Hettangian (upper Megastoma and lower Marmorea Zone in the Alpine zonation).

3.3. Bakony (Kőris-hegy)

The stratigraphy of the TJB transition in the Bakony Mts. is similar to the Gerecse and Tata in the Upper Triassic, but differs in the lowermost Jurassic as the Dachstein Fm. here is overlain by the Kardosrét Fm. The best exposure of the TJB strata is an artificial trench on the south slope of Kőris-hegy (47°16′59.83″ N, 17°45′18.99″ E), exposing c. 25 m of strata across the boundary. The topmost 12 m of the Dachstein Fm. dominantly comprises beds of member C of the Lofer cyclothems, thin beds of member A and B occur only sparsely. The Dachstein Fm. is locally cut by two steep neptunian dykes. Some beds yield megalondontid bivalves. The TJB is expressed by a contrast in color across a nearly planar surface. The lowermost Jurassic Kardosrét Fm. is thick-bedded, grey, yellow, and pink in color, and contains rare macrofossils (gastropods and brachiopods). The Kőris-hegy section was briefly described by Császár and Oravecz-Scheffer (1987).

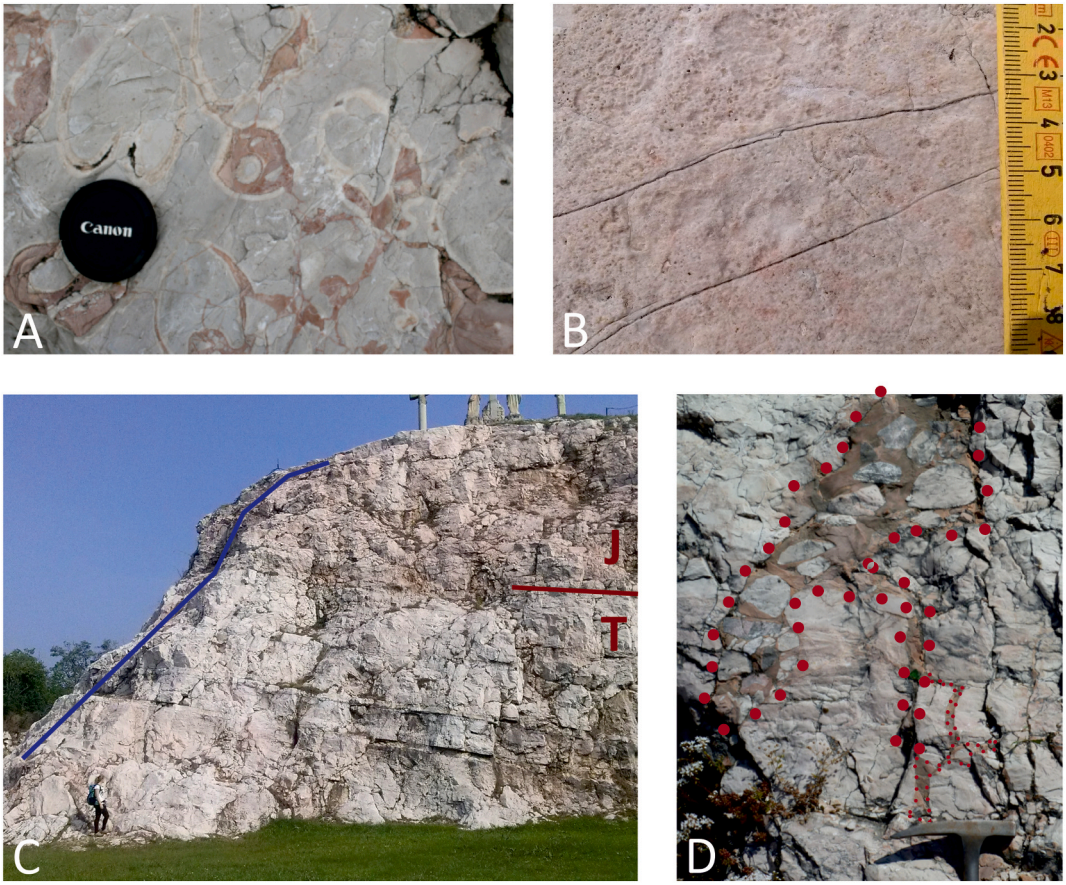

Fig. 5. The TJB in the Tata (Kálvária-domb) section. (A) Molds of megalodontid bivalves and irregular cavities filled by red micrite, surrounded by isopachous white fibrous calcite cement. (B) Densely spaced, rounded, shallow depressions, 0.5–2.5 mm in diameter, interpreted as borings on the top surface of Dachstein Fm. (C) View of the quarry wall showing the position of TJB and location of the profile sampled for stable isotope analyses. (D) Wide neptunian dyke (dotted outline) with micritic infill and broken clasts cutting through the topmost Rhaetian Dachstein Fm. (Photos A and D by Orsolya Győri.) (For interpretation of the references to color in this figure legend, the reader is referred to the web version of this article.)

4. Material and methods

4.1. Carbonate petrography

More than 30 thin sections of 5 × 5, 7 × 7 and 10 × 7 cm size were made from samples in the three measured sections; the larger-sized ones were especially useful to study the TJB surface across the top of the Dachstein Fm. At Tölgyhát and Vöröshíd, TJB samples were obtained using a drill corer. Archive thin sections of each bed of the Kőris-hegy section, made during the 1980's effort of documenting key stratigraphic sections in Hungary by the Geological Institute of Hungary, were made available to us and restudied. Petrographic descriptions follow the textural classification scheme of Dunham (1962). On the basis of component grain types and their abundance distribution, matrix type, sedimentary structures and fossils, samples were assigned to standard microfacies (SMF), using the 26 SMF types distinguished by Flügel and Munnecke (2010).

4.2. Stable isotope geochemistry

In the Vöröshíd quarry, the topmost 9 m of the Dachstein Fm. was sampled on average at 50 cm intervals, more densely near the TJB, whereas 20 cm spacing was used in sampling the lower 8.5 m of the Pisznice Fm., comprising its lower, thick-bedded unit. The sampled profile is located approximately at the northern third of the rock face in the upper quarry yard (Fig. S1).

In Tata, the TJB profile beneath the Calvary statue (Fig. 5C) was sampled at a 50 cm spacing in the uppermost 12 m of the Dachstein Fm. Beds of member B were avoided and 21 samples were obtained from member C beds only; sampling density was increased immediately below the boundary. The lower 5.6 m of the Pisznice Fm. was sampled uniformly at every 20 cm. In addition, two samples of Jurassic neptunian dyke fill (Fig. 5D) within the Dachstein Fm. were also collected.

From Kőris-hegy, a first sampling effort in 2007 obtained 43 samples from 20.5 m of the stratigraphic section. This was supplemented by additional samples from the upper 4.5 m of the Kardosrét Fm. exposed here.

In total we analyzed 164 bulk carbonate samples for $\delta^{13}C_{carb}$ and $\delta^{18}O_{carb}$ at the Institute for Geological and Geochemical Research (IGGR, Budapest, Hungary). After cutting and cleaning the samples we targeted and drilled the most homogeneous micritic fraction. Stable carbon and oxygen isotope compositions were determined by reacting carbonate powder samples (150–200 μg) with orthophosphoric acid at 72 °C (Spötl and Vennemann 2003) and analyzing the evolved CO_2 by an automated GASBENCH II sample preparation device attached to a Thermo Finnigan Delta Plus XP isotope ratio mass spectrometer (IRMS). Three laboratory standards calibrated with the NBS-18, NBS-19 and LSVEC standards (provided by the International Atomic Energy Agency) were used for inter- and cross-laboratory standardization. A Harding Iceland Spar (Landis 1983) sample was measured as unknown in the course of the study, and yielded $\delta^{13}C$ and $\delta^{18}O$ values of −4.92 ± 0.09‰ and − 18.50 ± 0.09‰ ($n = 28$), respectively. These values are close to the published values of −4.80 and − 18.56‰, respectively (Landis 1983). On the basis of these results, the accuracy and reproducibility of $\delta^{13}C$ and $\delta^{18}O$ values

are better than ±0.1‰.

Stable isotope curves were compiled from 62, 50, and 50 measurements on samples from the sections of Vöröshíd quarry, Tata, and Kőrishegy, respectively. Additional data were obtained from Tata, where two samples that represent the Jurassic infill of neptunian dykes were measured, to supplement results of a previous study of Győri (2014) that reports data from seven analyses partly also from neptunian dykes and partly from vugs in the Triassic limestone filled with Jurassic micrite.

4.3. Cyclostratigraphy

In a previous study, the 10 m thick lower, massive to thick-bedded part of the Pisznice Fm. that directly overlies the TJB surface in the Kálvária-domb section at Tata was subjected to detailed and high-resolution carbonate microfacies analysis using thin sections made perpendicular to bedding at 5 cm sampling interval (Fülöp 1976). From the abundance distribution of components in 200 successive thin sections plotted in text-fig. 20 in Fülöp (1976), we digitally read values of *Globochaete alpina* (spherical calcified planktonic green algae, Flügel and Munnecke 2010), sum of foraminifera, sponge spicules, crinoids, gastropods and ostracods, using Webplot Digitizer. These six time series from the raw data was supplemented by calculated ratios of sponge spicules to crinoids, *Globochaete*, and ostracods, and gastropods to *Globochaete*. For cyclostratigraphic analysis, these datasets are regarded to result from even-spaced channel sampling that represent continuous time series. Analyses were performed using the Acycle software (Li et al. 2019). Time series were checked for outliers, removal of no more than five outlier values were needed in any of the datasets, omitted data was substituted by interpolation to 5 cm. To avoid zero values in time series, in such cases 1 was added to each value to allow log-transformation. Sponge spicule, gastropod and ostracod datasets and the ratios were log-transformed. For detrending either the LOWESS (at 35%) or LOESS

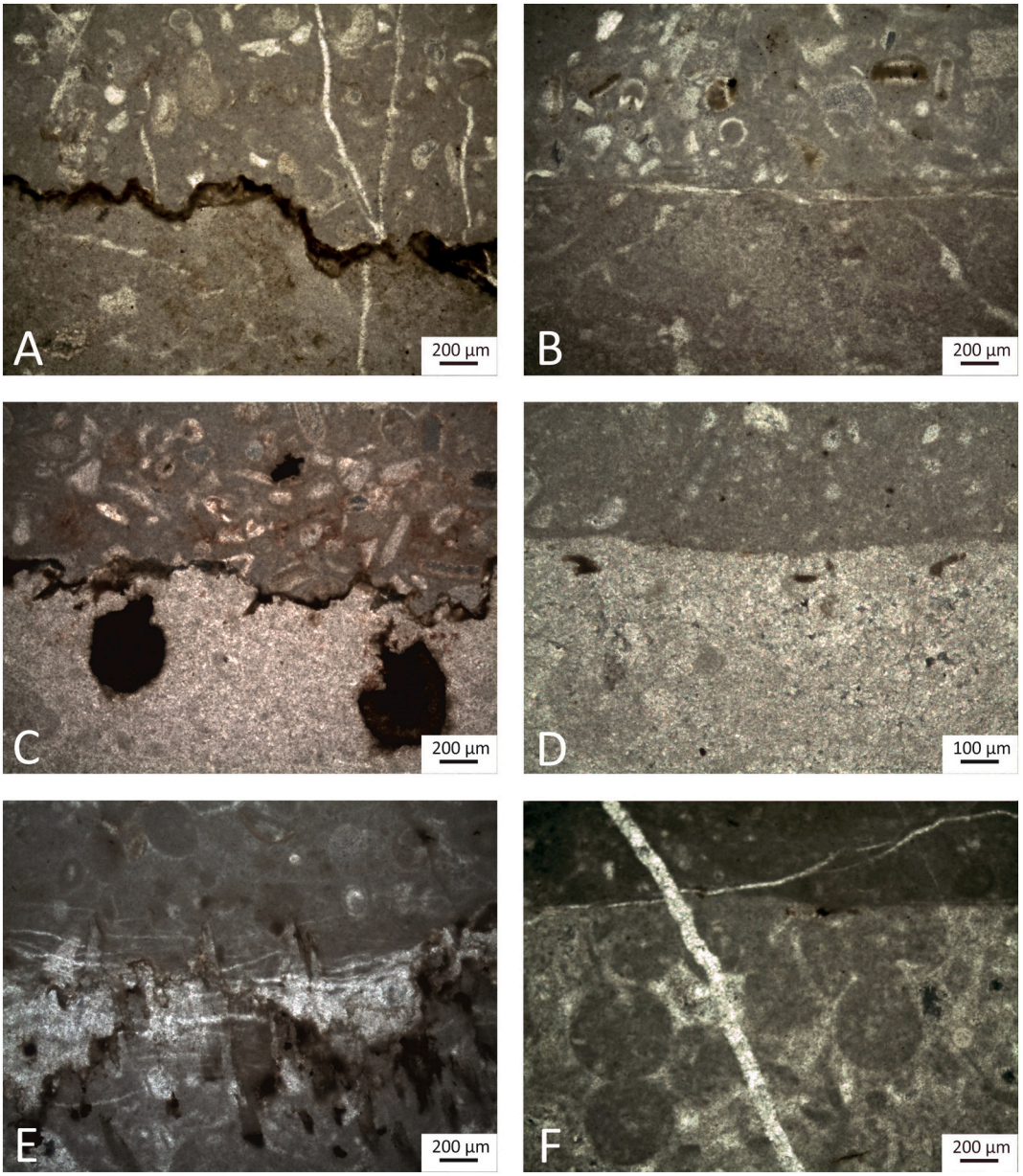

Fig. 6. Photomicrographs of various features observed at the TJB surface in the studied sections. (A) Clay residue along the TJB surface enhanced by pressure-solution (Tölgyhát). (B) Calcite cement precipitated along the sharp, planar TJB surface (Tölgyhát). (C) Wavy, stylolitic TJB surface coated with insoluble residue, with borings of c. 400 µm diameter immediately beneath (Pisznice). (D) Elongated borings of c. 100 µm length beneath and parallel to the TJB (Pisznice). (E) Columnar, serrated stylolytic TJB surface with calcite cement precipitates (Vöröshíd). (F) Crustacean fecal pellets truncated at the TJB surface (Kőris-hegy).

(at 40%) trend was removed from the time series. Power spectral analysis used the 2π multi-taper method (MTM) (Thomson 1982, 1990) and zero-padding. Confidence levels were calculated using the robust version of autoregression model. Construction of spectrograms (evolutionary power spectra) employed a sliding window of 380 cm and 5 cm steps. Band-pass filtering was carried out for each time series using the Gauss algorithm on the lowest-frequency cycle. Wavelet analysis was used to test for possible stratigraphic gaps.

5. Results

5.1. Characteristics of the TJB boundary surface

Microscopic features of the top boundary of the Dachstein Fm., that represents the TJB, display both similarities among and some differences between the studied sections. At Tölgyhát, the formation boundary is at some places stylolitic where the amplitude of surface irregularities is up to 200 μm. The thickness of the residual clay layer at the pressure solution surfaces is 50–100 μm (Fig. 6A). Carbonate component grains in the Pisznice Fm. are damaged at the stylolitic surface. Elsewhere the contact is gently undulating, nearly planar, and bears a thin cement layer (Fig. 6B). Multiple styles of the boundary surface also characterize the locality of Nagy-Pisznice, where contrasts may occur within a single thin section. Pressure solution is expressed in wavy or serrated stylolites of 200–600 μm amplitude, whose surface is coated with 25–100 μm thick brown dissolution residue (Fig. 6C). Overprint of the original surface and solution affected the integrity of components in the Jurassic carbonate. Elsewhere the boundary surface is planar or only mildly undulating, with a relief not exceeding 2 mm, and lacks stylolites and clay coating (Fig. 6D).

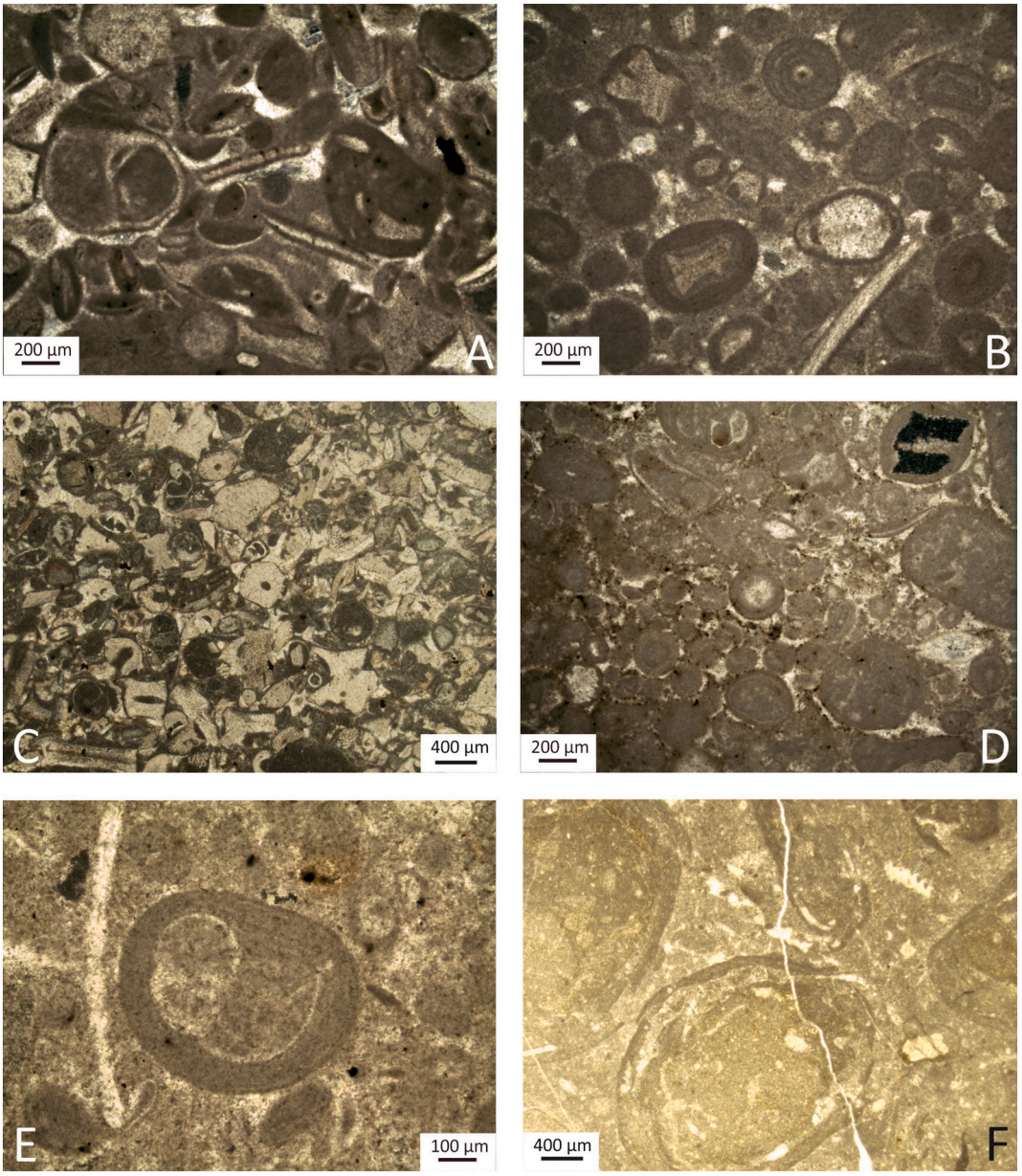

Fig. 7. Photomicrographs of various microfacies features observed in the basal Jurassic beds in the studied sections. (A) Bioclastic wackestone with common micritic envelope around bioclasts and rounded intraclasts (Tölgyhát). (B) Ooidal-peloidal packstone with micritised ooids, occasionally with concentric laminae (Tölgyhát). (C) Bioclastic packstone, with predominant echinoderm (crinoid) bioclasts, commonly surrounded by a thin micritic envelope (Pisznice). (D) Rounded intraclasts (0.4–1.2 mm in diameter), micritic clusters, micritized ooids (e.g. in upper right corner), and peloids as characteristic components (Vöröshíd). (E) Micritized ooid nucleated around a bioclast (Vöröshíd). (F) Oncoids with wavy laminae containing recrystallized bioclasts but no nucleus (Kőris-hegy).

Irrespective of the presence of stylolites, two types of burrows occur immediately below the boundary surface, not penetrating beyond 600 μm in depth. One type is circular in cross-section, 200–400 μm in diameter (Fig. 6C). Their ferruginous infill is not homogenous, their lining is darkest in color and contains angular fragments of ~10 μm with lighter and darker colored patches. The other type is smaller, elongated along the boundary surface or at a shallow angle reaching a length of 50–150 μm, also with a circular cross section of 25–30 μm and with ferruginous infill (Fig. 6D).

At Vöröshíd, the original boundary surface is entirely overprinted by pressure solution. The largest height (200–250 μm) of the columnar and serrated stylolites was observed here. The surface is marked by a thin coating of dissolution residue, enveloped within 200–600 μm thick layers of calcite cement (Fig. 6E).

At Kőris-hegy, the TJB surface is gently undulating, nearly planar. In the topmost Triassic, some of the components, both bioclasts and cement, are truncated, but those in the basalmost Jurassic are intact (Fig. 6F). Microborings are less common here than at Nagy-Pisznice. They reach a depth of 150 μm or remain subparallel to the boundary surface, and contain brown, ferruginous infill.

5.2. Carbonate petrography of the basal Jurassic strata

Above the TJB unconformity, the lowermost bed of the Pisznice Limestone at each section in the Gerecse consists of bioclastic wackestone that contains, in order of decreasing abundance, corroded crinoid fragments, gastropods, benthic foraminifera, ostracods, bivalve and brachiopod shell fragments. The large bioclasts are commonly surrounded by a micritic envelope (Fig. 7A). Densely bioclastic packstone occurs locally and may become more common in the next higher beds (Fig. 7C), transitioning to bioclastic grainstone texture. Bioerosion is also common. Still close to the TJB encrustation of grains (Fig. 7E) and intraclasts (Fig. 7D) appear and increase in abundance higher up. Sponge spicules and *Globochaete* also occur, the latter exhibits an upward increasing trend with fluctuation. Still within the first meter above the TJB, ooids appear, also as encrusted grains (Fig. 7B). Higher they become more abundant as ooidal peloidal grainstone or ooidal packstone becomes the characteristic microfacies. Several meters above the TJB, a gradual onset of dominance of bioclastic wackestone and a drop in abundance of echinoderms, gastropods, and benthic foraminifers are observed.

At Kőris-hegy, the lowermost Jurassic Kardosrét Limestone also contains common bioclasts of crinoids, ostracods, gastropods, and benthic foraminifers, along with rarer bivalves, brachiopods and sponge spicules. A distinctive difference is the dominance of coated grains of different origin. The most common among them are large (0.2–0.8 mm), poorly preserved, irregularly rounded oncoids of undulating outline, only rarely nucleated around bioclasts (Fig. 7F). Smaller-sized (300–400 μm) ooids are less abundant. The space between these grains is filled by microspar and peloidal cement. Throughout the first meters above the TJB, the dominant microfacies is oncoidal-ooidal packstone, locally with oncoidal-bioclastic wackestone. A more detailed description of the microfacies of basal Jurassic strata in each section is given in the Supplementary material.

5.3. Stable isotope chemostratigraphy

5.3.1. Vöröshíd

The stable isotope curves, constructed of measurements of 62 samples from a 17.5 m thick stratigraphic interval, display marked differences below and above the TJB (Fig. 8, Table S1). Overall, carbon isotope values fall in the range of 1.2–2.6‰. The uppermost Triassic is characterized by a narrower range (1.9–2.6‰) with an average value of 2.3‰, whereas the range of values is wider (1.2–2.4‰) and their average is lower (1.9‰) in the lowermost Jurassic. In the Dachstein Fm. there is no trend but cyclic meter-scale oscillations of up to 0.5‰ occur throughout. The most prominent feature of the curve is a sharp drop of 1.3‰ in the lowermost samples immediately above the TJB. From this minimum an overall positive trend is present in the more densely sampled Hettangian, overriding subdued cyclic oscillations.

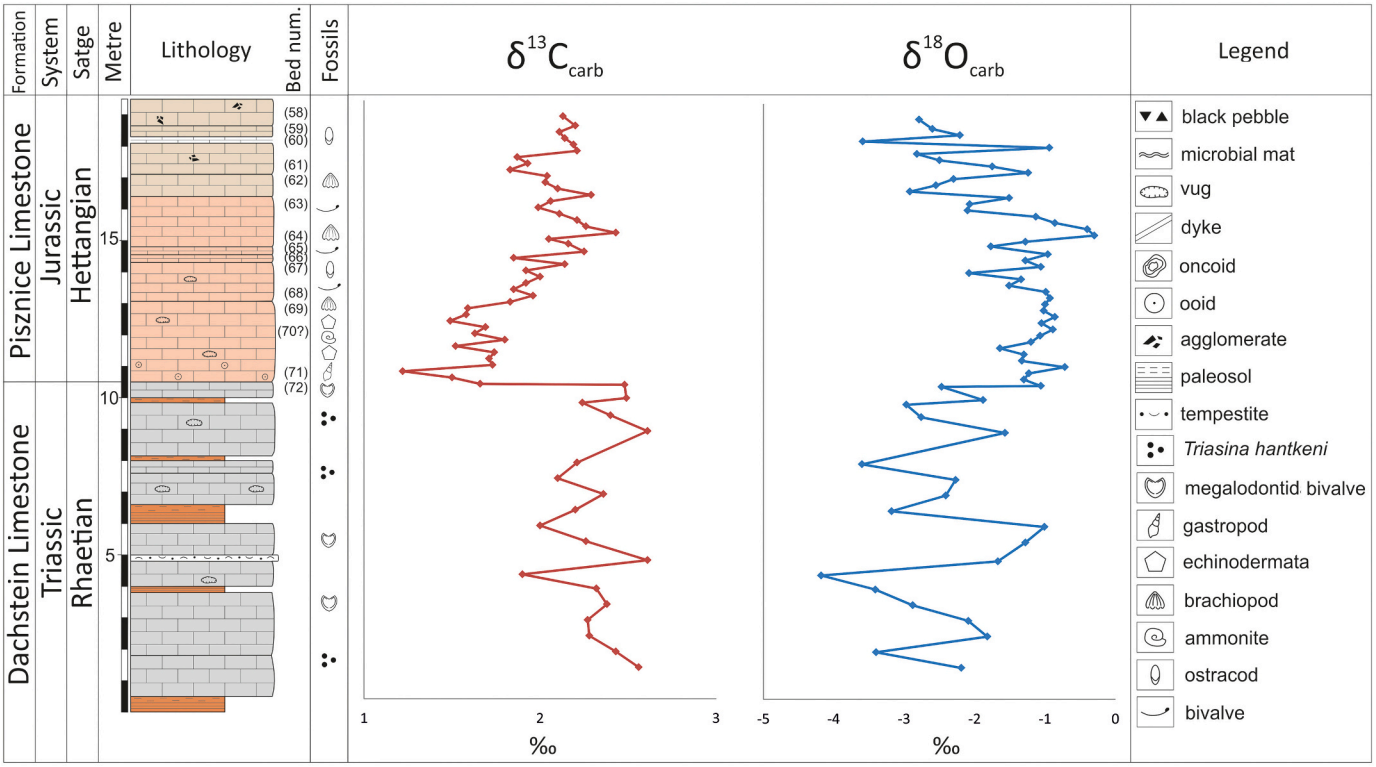

Fig. 8. Stratigraphic and lithologic log of the Vöröshíd section along with stable C and O isotope curves.

Although the oxygen isotope curve is noisier (within a range of −4.2 to −0.3‰), its Rhaetian part is similar to the carbon curve in the presence of large oscillations (up to 3‰), and it shows a weak positive trend. The lowermost 5 m in the Jurassic exhibits slightly less negative and more stable values with no clear trend, followed by an interval of larger oscillations (up to 1.7‰) overriding a negative trend.

5.3.2. Tata

The stable isotope curves, constructed of measurements of 50 samples from a 15.6 m thick stratigraphic interval, are characterized by significant differences below and above the TJB (Fig. 9, Table S1). Carbon isotope values fall in a range of 0.2–2.9‰ with an average of 2.1‰ within the uppermost Triassic, whereas they remain within a narrower range (0.2–2.4‰) with a similar average (2.0‰) in the lowermost Jurassic. In the Dachstein Fm. three cycles of marked oscillations with prominent minima occur. However, the topmost 2.5 m shows only slight fluctuation with values around 2.7‰. A negative shift of 0.9‰ marks the TJB, followed in the Hettangian by stable values in the lowermost 1.5 m, a gradual positive shift of 0.7‰ upsection, then again stable values around 2.2‰ (except for a negative outlier at 4.2 m above the TJB). Two samples from neptunian dyke fills of red micrite of assumed Jurassic age yielded carbon isotope values (1.8‰ and 2.0‰) close to the observed average, and oxygen isotope values (−0.1‰ and 0.4‰) that are marginally heavier than those obtained in the basal Jurassic part of the section.

The oxygen isotope curve is similar to the carbon curve in its oscillations (within a range of −3.9 to −0.5‰) in the Rhaetian but shows little change across the TJB. The flat trend and near constant values with only minor fluctuation from the topmost Dachstein Fm. to the basal Pisznice Fm. change at 3.8 m above the boundary to an oscillatory pattern with 1–2‰ in amplitude.

5.3.3. Kőris-hegy

Stable isotope curves have been constructed from measurements of 50 samples taken from a nearly 20 m thick stratigraphic interval (Fig. 10, Table S1). Half of the samples were obtained from the topmost 13.35 m of the Dachstein Fm., the other half from the more densely sampled lowermost 6.5 m of the Kardosrét Fm. Overall, carbon isotope values vary between −0.8 and 2.6‰. Oscillations are more pronounced in the Rhaetian part which is also characterized by a more positive average value of 1.6‰. The average from the Hettangian Kardosrét Fm. is 0.7‰, i.e. nearly 1‰ isotopically lighter than in the Triassic, and a shift to lower values is apparent across the TJB. The lowest values in the Dachstein Fm. at 4.2 m were obtained on samples from a member B of Lofer cyclothems. A negative peak supported by multiple successive samples over a nearly 2 m interval in the Hettangian occurs 3.4 m above the TJB, with a minimum of −0.8‰, some 1.7‰ lower than the Hettangian background value.

The oxygen isotope curve exhibits multiple large oscillations in the Rhaetian, with amplitudes up to 1.6‰ and within a range of −3.7 and 1.7‰. Fluctuations in the Hettangian remain within a narrower range and the average in the Jurassic part of the section is −2.5‰, 0.5‰ lower than in the Triassic. A negative peak, c. 1.3‰ below the Hettangian background, occurs at the same stratigraphic level as the similar peak in carbon isotopes.

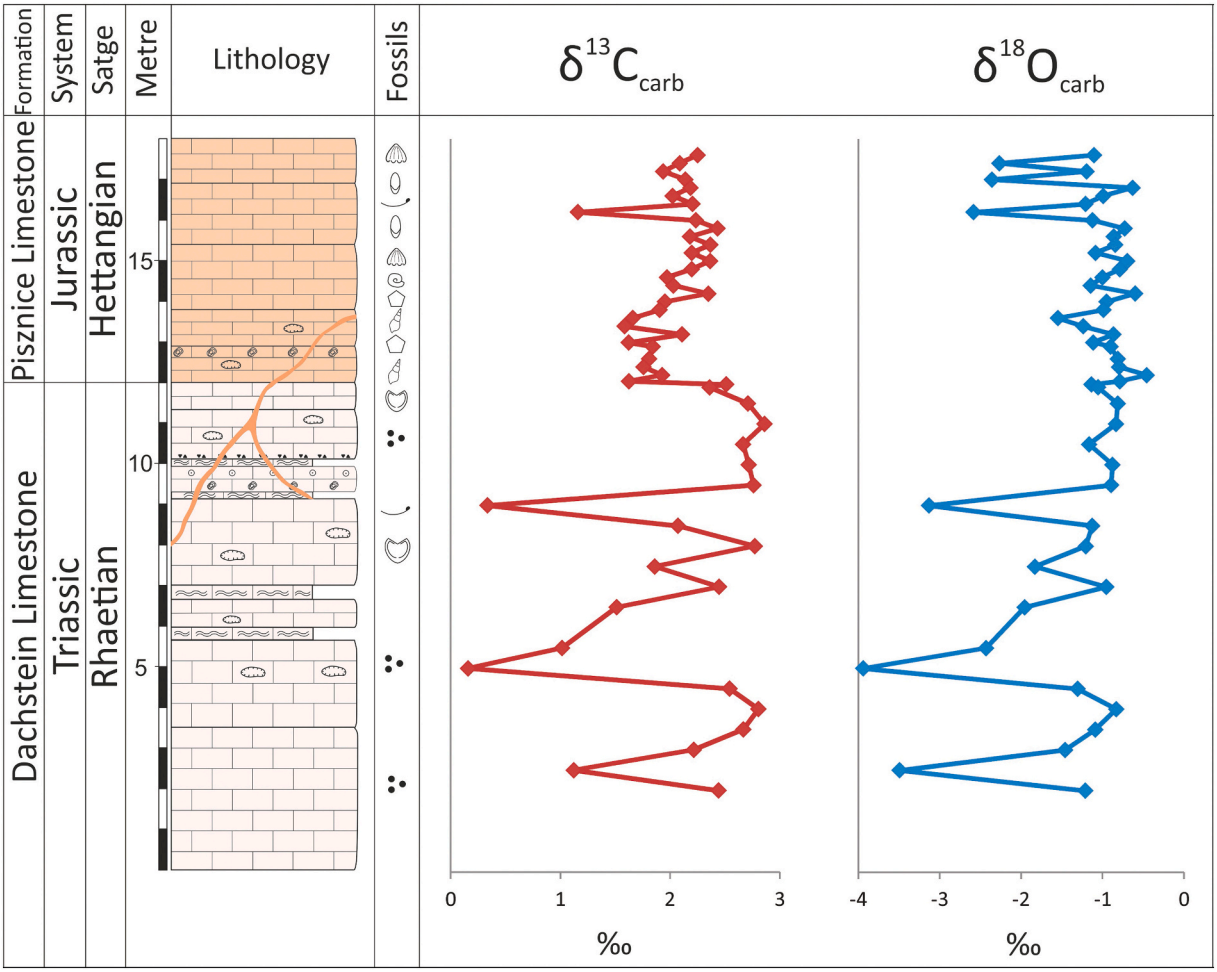

Fig. 9. Stratigraphic and lithologic log of the Tata (Kálvária-domb) section along with stable C and O isotope curves. For legend, see Fig. 8.

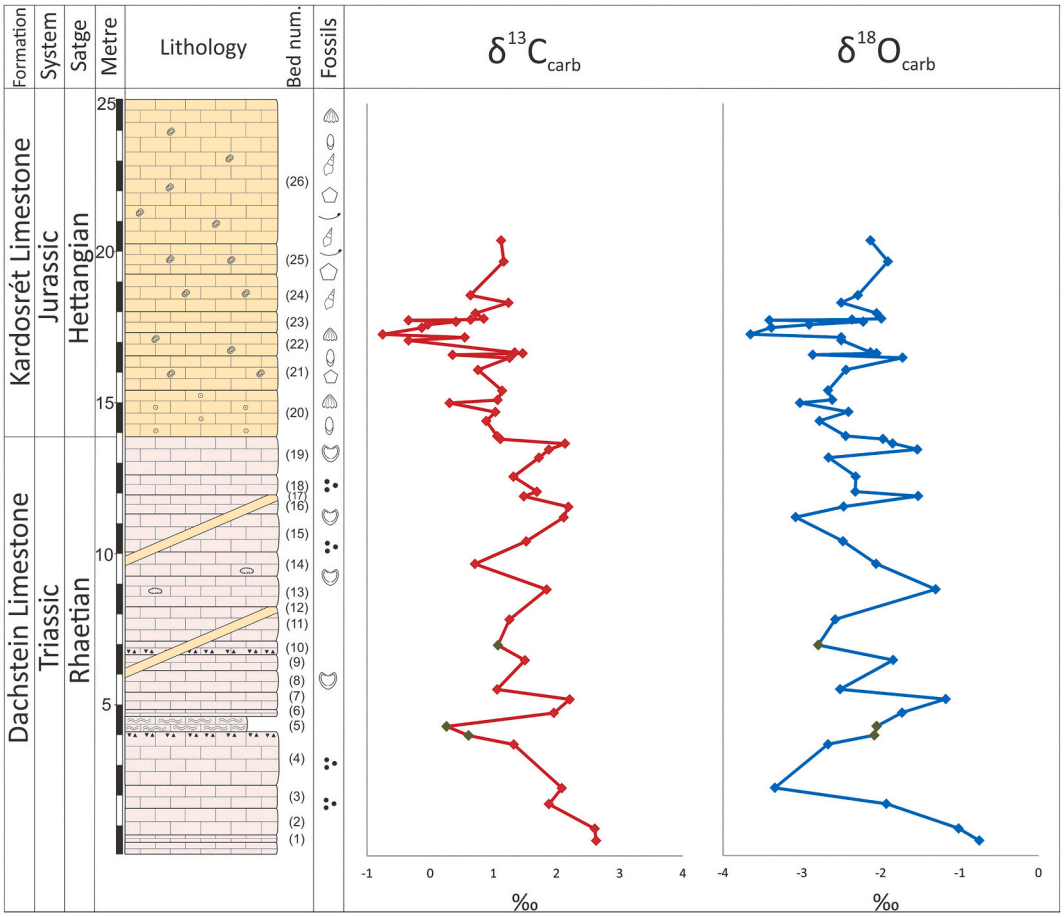

Fig. 10. Stratigraphic and lithologic log of the Kőris-hegy section along with stable C and O isotope curves. For legend, see Fig. 8.

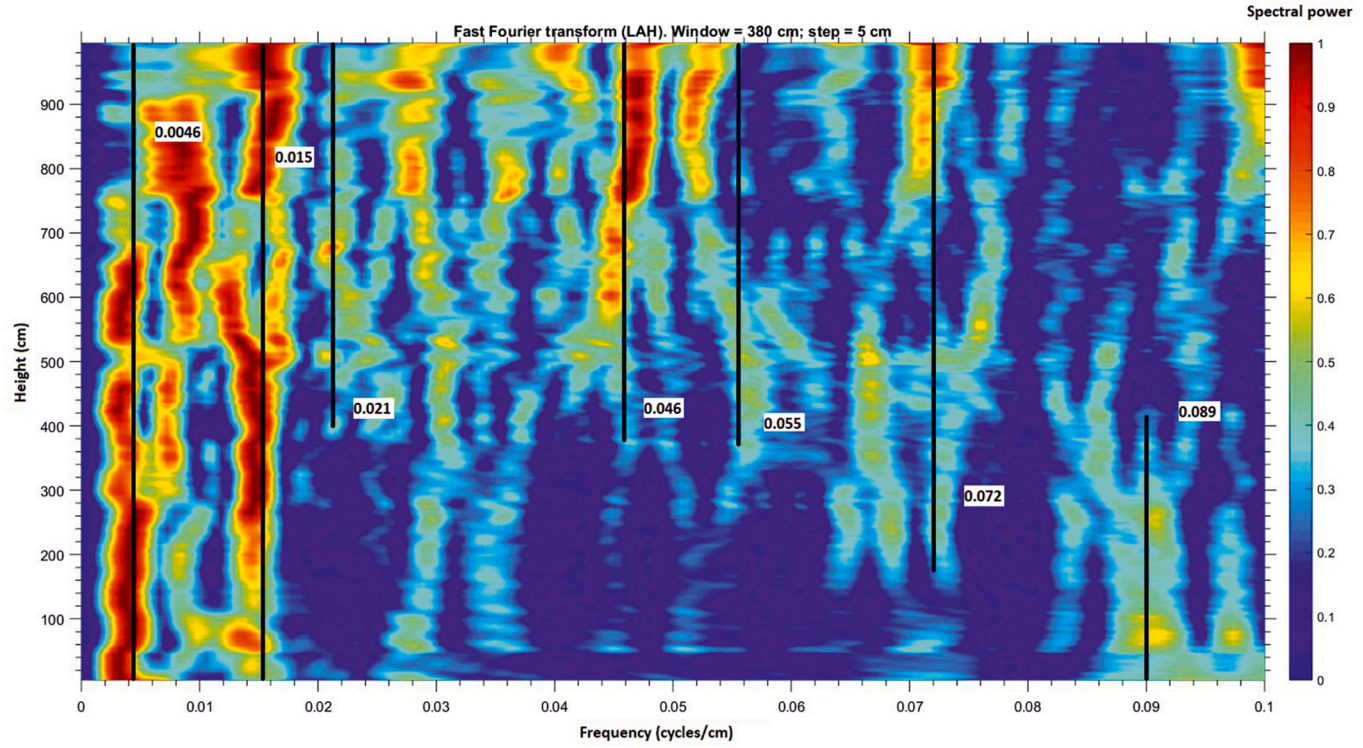

Fig. 11. Spectrogram and recognized periodicities of the sponge spicule abundance time series from the lower 10 m of Pisznice Formation in the Tata, Kálvária-domb section. Data from Fülöp (1976).

5.4. Cyclostratigraphy

Although all of the analyzed time series are somewhat nosiy (see text-fig. 20 in Fülöp 1976), there are six different cycle frequency ranges where most of the time series display detectable periodicity. Considerable variations are present among the different proxies and stratigraphic intervals, as well as the exact position of peaks within each frequency range. However, detailed comparison of power spectra, spectrograms, and related F-tests allowed determination of the most likely frequency values, except for the highest one where only a likely range was identified (6.9–7.4 cycle/m or 0.069–0.074 cycle/cm) (Table S2). Sponge spicules, crinoids, ostracods and their respective ratios yielded the most reliable results. Spectrograms display quasi-linear bands related to the different periodicities, although the signal is weaker in the lower 3–4 m than higher upsection (Fig. 11). Presence of Milankovitch periodicities is demonstrated by the ratio of observed frequencies, considering the generally accepted period lengths for the Triassic-Jurassic transition (Laskar et al. 2004; Hinnov and Hilgen 2012). Equating the lowest frequency cycle (0.46 cycle/m) with long eccentricity, it follows that frequencies of 1.5 and 2.1 cycle/m correspond to dominant periodicities of short eccentricity, whereas 5.5 cycle/m represents the dominant obliquity. The other two, albeit weaker obliquity components are 4.6 and 6.9–7.4 cycle/m (Table S3). It follows that the expected frequency of precession cycles are near the Nyquist frequency which is 10 cycle/m in this dataset. The predicted frequency of the 21 kyr precession from the ratio method is 0.089 and it appears to be present in some time series (e.g. sponge spicules, foraminifera, *Globochaete*) but only with low signal-to-noise ratio. The shorter precession periodicity (17 kyr) signal is not detectable as it falls below the Nyquist frequency. The averaging effect of channel sampling cancels out aliasing but, on the other hand, it may also be responsible for weak preservation of the precession signal.

For band-pass filtering, we assumed that the 0.46 ± 0.06 cycle/m frequency represents the long-eccentricity periods, then these stable 405 kyr cycles were fitted to the signal. Although neither of the analyzed time series is perfectly preserved, the calculated total duration remains within a reasonably narrow range between 1.658 and 1.947 Myr, with an average of 1.784 Myr (Table S4). Remarkably, the sponge spicule time series (and ratios derived from it) are in antiphase with all other time series, which in turn are in phase with each other. Accumulation rates calculated from these duration estimates range from 5.13–6 m/Myr. Although wavelet analysis also yielded somewhat noisy results (Fig. S3), it helped confirm the lack of frequency switch between periodicities (also evident from the spectrograms) that indicates stability of depositional rate. The wavelet spectrogram does not reveal any hidden gaps in the analyzed 10 m thick stratigraphic interval.

6. Discussion

6.1. The TJB surface and facies contrast

In each of the studied sections the TJB is marked by a sharp disconformity surface that separates lithologically distinct units with different bedding attributes, color and texture. Prominent presence of Lofer cycles in the uppermost Triassic Dachstein Fm. and the lack of visible cyclicity above the TJB is a first-order feature most easily observed in the field. Interpretation of such discontinuity surfaces need to be based on small- and large-scale stratal geometry, lateral extent, facies contrast, differences in diagenesis, and age (Hillgärtner 1998). Observations of the TJB in our study are summarized in Table 1.

Several features hint at development of submarine hardgrounds which formed on the seafloor due to early marine cementation. Their genesis could be related to reduced sedimentation rate, removal of sediment in high energy environment, or physico-chemical submarine erosion (Christ, 2015). A diagnostic feature is the presence of micro- and/or macroborings, caused by activity of either bivalves, sponges, algae or fungi (Flügel and Munnecke 2010). Both macro- and microborings (Figs. 3B, 6C) occur at Pisznice. Macroborings at Tata form a dense network (Fig. 5B), at Pisznice their ferruginous infill is also characteristic to hardgrounds. Although ferruginous crust is common on hardgrounds with long exposure in low-energy seafloor, it does not occur in the studied sections, in agreement with the high-energy, shallow marine environment inferred from nearly planar or only slightly undulating morphology and lack of encrusting organisms. Microfacies features at Kőris-hegy, such as microborings, isopachous calcite cement surrounding fecal pellets and algal components, and truncation of bioclasts, fecal pellets and cement (Fig. 12) also point to early marine lithification. Truncated megalodontid molds at Vöröshíd and Tata are expression of the same phenomenon at the macro-scale. A distance of 65 km between sections displaying features or submarine lithification attest to the regional extent of environmental changes (Hillgärtner 1998).

Although a submarine exposure interval may have been preceded by subaerial exposure, for the latter there is no unambiguous evidence, such as karstification and pedogenesis, either in morphology, isotopic signal or petrographic features. Even admitting a preservational bias against it, terrestrial exposure, if there was any, could not have been prolonged if no trace of it remained.

Features of Early Jurassic resumption of sedimentation are consistent with a platform drowning event. Bioclasts are dominated by echinoderms and gastropods in each section except for Kőris-hegy, where these components also occur but bioclasts are less common. Cortoids, interpreted as biogenic encrustations, are common in all sections. Microborings on echinoderm fragments are common at Pisznice and Vöröshíd, and also occur at Kőris-hegy. These features are characteristic after platform drowning (Flügel and Munnecke 2010).

Drowning events and resulting unconformities commonly represent the response of shallow marine ecosystems to paleoceanographic and/or paleoenvironmental change (Godet 2013). Lowermost Jurassic strata in the studied sections offer keys to reconstruct the depositional environment of resuming sedimentation, enabling inference on the causes of platform drowning. Common occurrence of crinoids unequivocally suggests normal salinity. Indicators of high energy bottom waters include rounded intraclasts and micritic, concentric ooids at Tölgyhát and Vöröshíd. Besides bioclasts indicative of shallow water, the occurrence of *Globochaete* may signal more open marine conditions. Encrusted bioclasts, micritic envelopes and micritized grains, rounded intraclasts, peloids and ooids allow assignment to standard microfacies type SMF 11 that is characteristic to agitated waters above the fair-weather wave

Table 1
Observed features at and across the TJB and the top of the Dachstein Fm. in the studied sections.

	Tölgyhát	Pisznice	Vöröshíd	Tata	Kőris-hegy
Morphology of TJB surface	planar	planar, undulating	planar	planar	planar
Facies contrast	compositional	compositional	compositional	compositional	compositional
C isotope curve			1‰ negative shift	1‰ negative shift	1‰ negative shift
Biological activity		boring		boring	boring
Mineralization		slight Fe		slight Fe	
Clay		x			
Stylolytes	x	x	x		
Truncated components			x	x	x

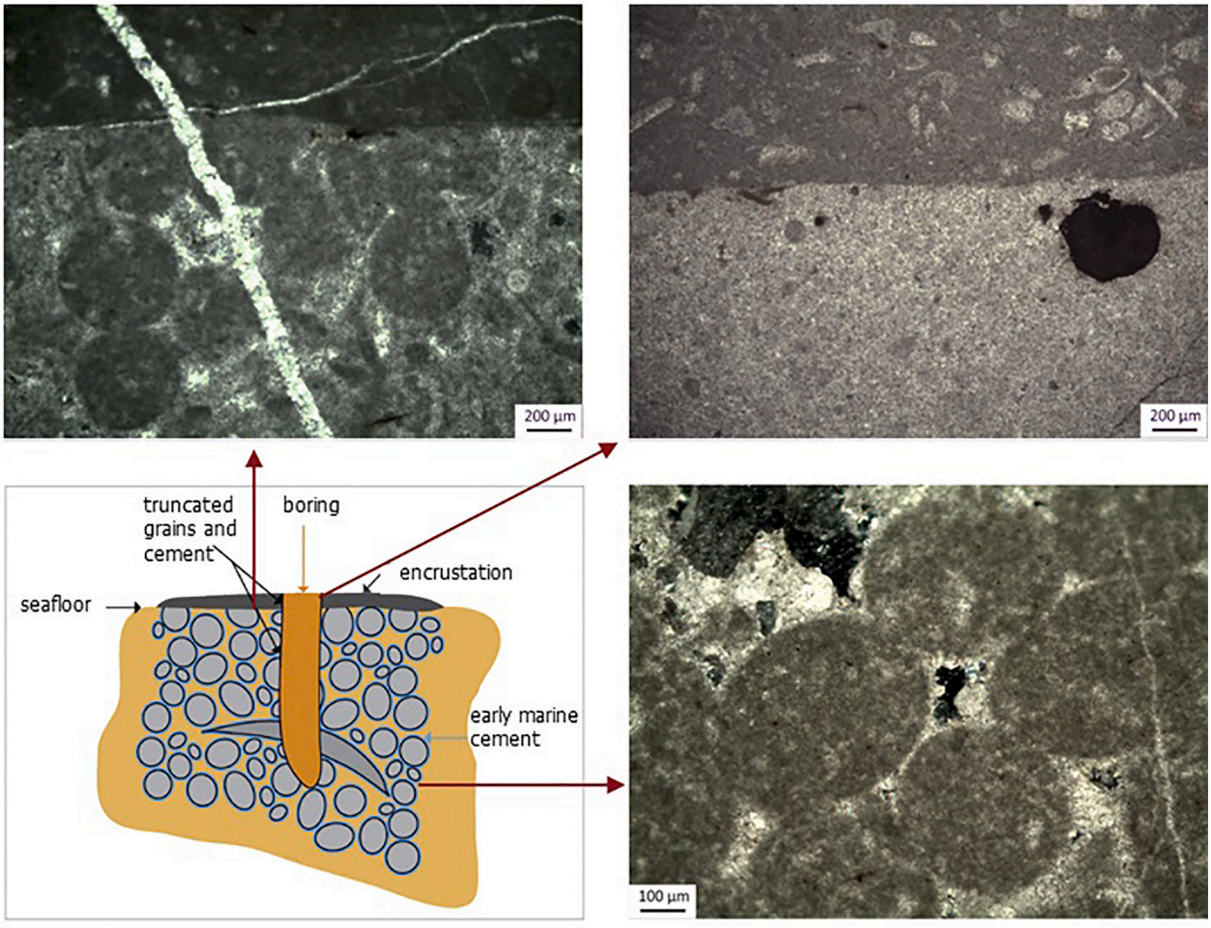

Fig. 12. Macro- and microscopic features hinting at early marine lithification and development of a submarine hardground at the TJB: truncated component grains (upper left), polyphase infill of a boring immediately below the boundary surface (upper right), and fibrous marine calcite cement enveloping crustacean fecal pellets (lower right). Conceptual model (lower left) adapted from Christ et al. (2015).

base or between that and the storm wave base (Flügel and Munnecke 2010). Cement spar is subordinate to micritic matrix, suggesting inner or mid-ramp depositional environment, as no surviving platform is known from the Gerecse Mts. Rarity of grainstone texture points to a leeward ramp where lime mud is expected to dominate.

Abundance of corroded and abraded crinoid fragments at Nagy-Pisznice also points to moderately agitated bottom as the optimal habitat of these filter feeding benthic organisms. Abraded and commonly encrusted bioclasts embedded in fine-grained matrix of packstone or wackestone texture are characteristic to SMF 10, formed in an inner to mid-ramp characterized by reworking from a higher to lower energy environment.

The lowermost Jurassic Kardosrét Limestone in the Bakony Mts. differs from the Pisznice Limestone in the Gerecse Mts. Apart from the basal bed, rounded oncoids are dominant in the lowermost Jurassic at Kőris-hegy, suggesting gently but continuously agitated bottom waters, supported by rarer ooids. Lack of orientation of ostracod shells is also consistent with this interpretation or, alternatively, they may have been stuck in microbial mats. Fine matrix is also in agreement with the low energy environment. Oncoids often indicate proximity of platform margin or migrating mounds of calcareous sand. The lack of rudstone and grainstone texture excludes a reefal setting and suggests either a protected environment behind a sand bar or zone of mounds, or a middle to outer ramp setting.

Previous authors also noted high energy depositional environment (Konda 1988) and the role of bottom currents for the Pisznice Fm. but envisaged a shallow marine basin of rather uniform depth. Substantial differences between the lowermost Jurassic of the Bakony and Gerecse Mts. were emphasized by Vörös and Galácz (1998), explained by the dissected topography of the disintegrating former platform. At a smaller scale within the Gerecse Mts., similar, fault-controlled differences of basin topography and bathymetry were invoked for the depositional model of the Pisznice Fm. (Császár et al. 1998; Budai et al., 2018).

Our observations confirm the higher energy depositional environment of the Pisznice Fm. in the Gerecse Mts. relative to the Kardosrét Fm. in the Bakony Mts. where the platform survived the TJB, albeit in a sedimentary regime that is noticeably different from the Late Triassic. However, we also reveal a spatial pattern of facies differences in the Pisznice Fm. that is more consistent with deposition in an inner and proximal mid-ramp setting rather than on a tectonically disintegrating drowned platform with pronounced bathymetric differences.

6.2. *Chemostratigraphic correlation of sections*

As age-diagnostic fossils are sparse in the Triassic Dachstein Fm. and the Jurassic Pisznice and Kardosrét Fm., stable isotope stratigraphy provides an alternative means of correlation of the studied sections. Before attempting chemostratigraphic correlation of the newly generated curves with other TJB sections, the possibility of diagenetic overprint needs to be assessed. Cross plots of carbon and oxygen isotopic composition of carbonates are informative as the latter isotope system is more prone to alteration after burial (Marshall 1992). Triassic and Jurassic samples are plotted separately for the three sections in Fig. 13. Significant correlation, a potential indicator of diagenetic overprint, is

only present in the Triassic samples from Tata ($r^2 = 0.9$) and Jurassic samples from Kőris-hegy ($r^2 = 0.58$). The latter may suggest that in that section the unique Hettangian negative $\delta^{13}C$ excursion may result from restricted occurrence of late diagenetic cement (Allan and Matthews 1982) at some stratigraphic levels and thus it is prudent not to consider it for correlation. However, Jurassic segments of the $\delta^{13}C$ curves from the other two sections are regarded to reflect primary variations of seawater isotopic compositions.

Fig. 14 illustrates C isotope curves from three sections (Vöröshíd, Tata and Kőris-hegy) plotted on the same scale and aligned at the TJB hiatus. In each case, the Triassic and Jurassic segments are clearly different but the correlation among the sections is remarkable. The uppermost Triassic parts of C isotope curves from both Tata and Kőris-hegy, and O isotope curves from all three sections are closely similar in their range of values and fluctuations. The largest amplitude of oscillation, on average 2.3‰ in $\delta^{13}C$, is observed in Tata. In each section, the stratigraphic spacing of isotope peaks is ~2.5 m, in concordance with the average thickness of Lofer cycles in the Dachstein Fm. in the Transdanubian Range (Haas and Budai 2014). Although our sampling strategy was designed mainly to establish a latest Triassic background for the characterization of any change across the system boundary, even at this coarse resolution there is a clear expression of Lofer cyclicity in the stable isotope record. In several cases, negative peaks correspond to intertidal and supratidal members B and A, respectively. Stable isotopes thus provide additional support for the genetic model of peritidal carbonate sedimentation on the Dachstein platform controlled by sea level fluctuations (Haas et al. 2007). Analogous meter-scale shallowing-upward cycles in peritidal carbonates at the TJB in Sicily (Mt. Sparagio) are similarly manifest in $\delta^{13}C$ oscillation (Todaro et al. 2018). Lower Cretaceous peritidal carbonates display similar isotopic signatures of facies-controlled cyclicity (Joachimski et al., 1994). In the Dachstein Fm., $\delta^{13}C$ values of subtidal carbonates of member C fall into the range of normal marine Rhaetian seawater, as established from brachiopod shells (Mette et al. 2012).

All three sections exhibit an abrupt negative shift of ~1‰ in $\delta^{13}C$ across the TJB unconformity and disappearance of cyclic oscillations in the lowermost Jurassic. Curves from Tata and Vöröshíd show further similarity in a gentle increasing trend above the lowermost 1.6 and 2.4 m, respectively, whereas a Hettangian negative excursion is only recorded in Kőris-hegy. These subtle differences suggest slight differences in timing of resumption of sedimentation after the TJB hiatus.

Distinctive changes in the carbon cycle around the TJB are widely used for chemostratigraphic correlation (Korte et al. 2019). The most salient feature is a short-lived and sharp negative carbon isotope excursion (CIE), termed the initial CIE (Hesselbo et al. 2002), coincident with the end-Triassic extinction. The lack of its expression in the studied sections is best explained by the hiatus at the TJB that could be causally linked to the same chain of events that led to the cessation of platform growth and submarine erosion as well as mass extinction and carbon cycle perturbation. The negative shift across the TJB may indicate that sedimentation resumed in the Hettangian during the main CIE, a prolonged negative excursion recognized in many but not all sections worldwide (Hesselbo et al. 2002). However, Hettangian $\delta^{13}C_{carb}$ records established from carbonates that formed in different shallow marine environments carry significant differences (e.g. van de Schootbrugge et al. 2008; Bachan et al. 2012; Ge et al. 2018; Todaro et al. 2018), that defy simple explanations and call for caution in chemostratigraphic correlation (Fig. 15). The new records presented here show the greatest similarity with a section in the western part of Northern Calcareous Alps (Steinernes Meer; Felber et al. 2015). Shared features include the lack of a preserved initial CIE, a negative shift that may be correlated with the upper part of the Hettangian main CIE above the TJB unconformity, and the rising limb of a Hettangian positive CIE that occurs in several other Tethyan sections (Fig. 15).

If the lack of preserved initial CIE is explained by the gap at TJB, the isotopic signature may offer additional clues to the genesis of

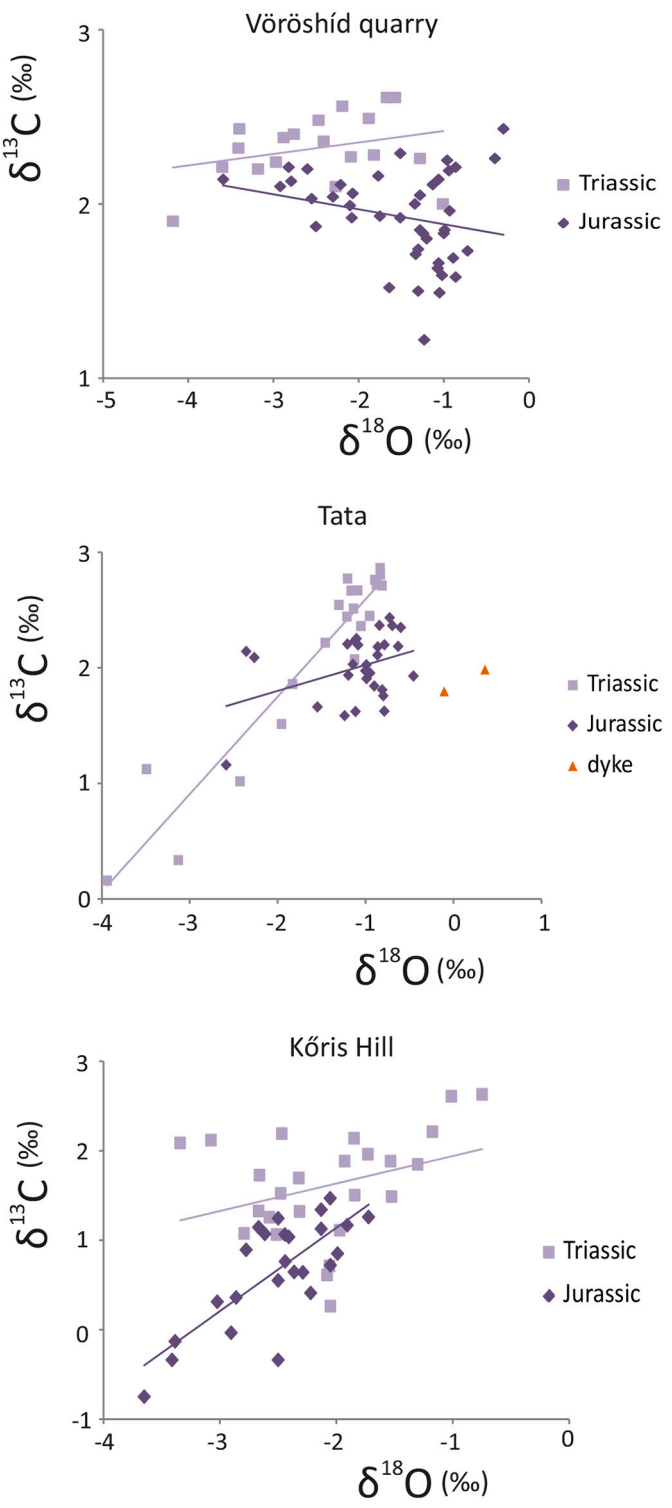

Fig. 13. Cross plots of stable C and O data from the sections of Vöröshíd, Tata and Kőris-hegy.

unconformity. An extended period of subaerial exposure would be expressed in a gradual negative $\delta^{13}C$ shift up to the unconformity, resulting from increasing effect of isotopically light carbon, sourced from terrestrial organic matter and delivered by downward flow of groundwater (Rameil et al. 2012). The lack of this feature in the studied sections provides an indirect evidence against long-term emergence at the termination of platform growth. Conversely, submarine hardgrounds are commonly characterized by a positive shift but only in the

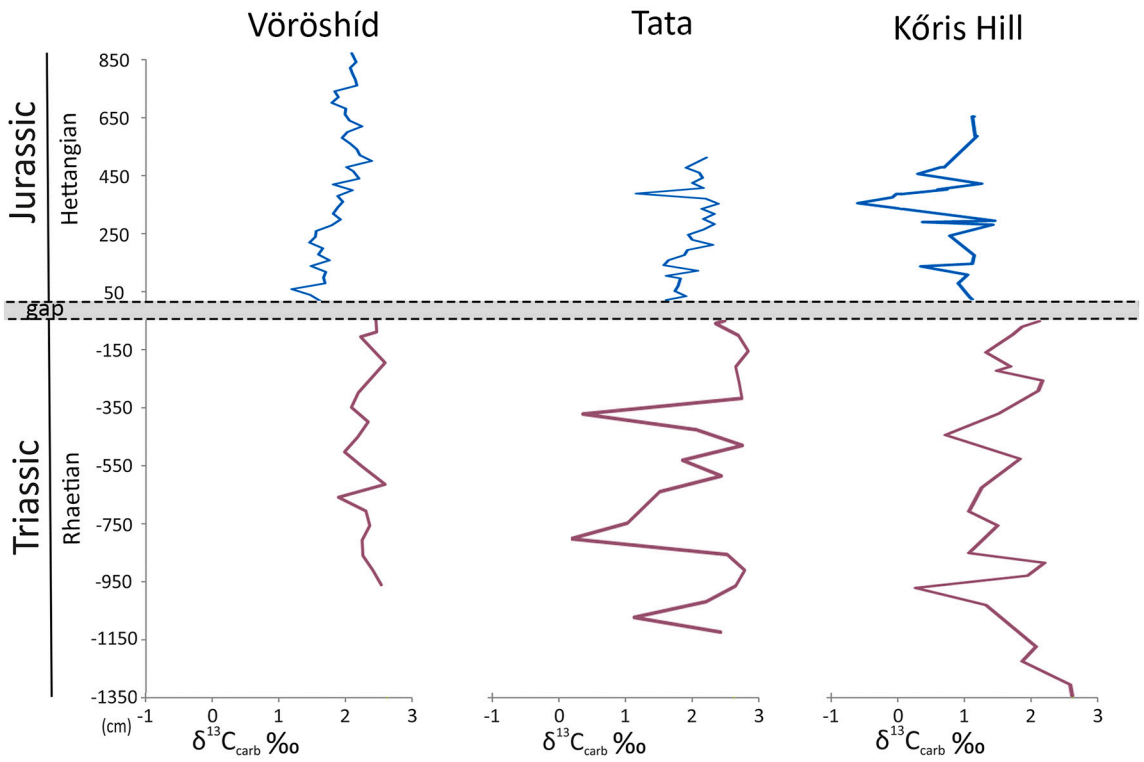

Fig. 14. Comparison of stable carbon isotope curves from the Vöröshíd, Tata and Kőris-hegy sections, plotted on the same stratigraphic scale and correlated at the TJB where the hiatus indicated.

uppermost 1–2 cm below the hardground (Godet et al., 2013), a resolution not attained in our sampling.

6.3. Estimating the duration of the TJB gap

Combination of available ammonoid biostratigraphy (Koch 1909; Szabó 1961; Géczy in Fülöp 1976; Pálfy et al. 2007) and the astrochronological age model developed here, together with published Hettangian numeric time scales, allow estimation of the length of the hiatus in the Tata, Kálvária-domb that helps constrain different models for the TJB events.

Despite the significance of the Kálvária-domb section for the Mesozoic stratigraphy in Hungary (Haas and Hámor 2001), ammonoid faunas and their biostratigraphy are less well studied compared to other Jurassic key sections in the Transdanubian Range. Although detailed, bed-by-bed collections are lacking, many specimens were acquired during decades of active quarrying. Already the early workers noted that lithological differences are reflected in fossil preservation (Koch 1909), permitting reliable assignment of taxa identified from museum specimens to stratigraphic units. Ammonites from the poorly bedded, 10 m thick Vöröshíd Member, that directly overlies the Dachstein Limestone Fm. and is in the focus of our study, yielded relatively poorly preserved internal molds of ammonites. Although Géczy (in Fülöp 1976) questioned the presence of Middle Hettangian that was suggested by both Koch (1909) and Szabó (1961) on the basis of *Alsatites perspiratus* and *A.* cf. *proaries*, recent field work by Pálfy et al. (2007) suggested the occurrence of mid-Hettangian genera *Discamphiceras*, *Alsatites* and *Kammerkarites* with specimens found in place in the lower few meters of strata. Thus only the Lower Hettangian cannot be proven by ammonites. The upper part of this unit contains diagnostic species of the Upper Hettangian Marmorea Zone, e.g. *Schlotheimia marmorea* and *Paracaloceras coregonensis* (Szabó 1961; Géczy in Fülöp 1976). The overlying unit, more distinctively bedded and darker pink to red in color (Nagypisznice Member), yielded better preserved specimens. The revision of Géczy (in Fülöp 1976) confirmed the presence of *Metophioceras conybeari* and other species of this genus which is a reliable indicator of the lowermost part of the basal Sinemurian Bucklandi Zone. The next higher Semicostatum Zone is also well represented in the ammonoid assemblage from this unit. Thus the top of the 10 m thick unit studied here by chemo- and cyclostratigraphy lies at the biostratigraphically defined Hettangian-Sinemurian boundary.

Current estimates for the duration of Hettangian stage are controversial. Biostratigraphically constrained U-Pb ages from volcanic ash beds near the TJB place the base of the Jurassic at 201.36 ± 0.17 Ma (Schoene et al. 2010; Wotzlaw et al. 2014) and the Hettangian-Sinemurian boundary at 199.53 ± 0.29 Ma (Schaltegger et al. 2008; Guex et al. 2012). A similar duration of 2.0 (± 0.5) Myr is suggested in the current Geological Time Scale (Ogg et al. 2016), derived from these U-Pb ages and astrochronology of sections in SW England. There, the St. Audrie's Bay and Quantoxhead sections are well calibrated by ammonoid biostratigraphy (except for the undocumented lowermost Hettangian Tilmanni Zone) and yielded a duration of 1.8 Myr for the Hettangian (Ruhl et al. 2010a; Hüsing et al. 2014). However, this view was challenged by Weedon et al. (2019) who compiled a cyclostratigraphic composite with horizon-level ammonoid biostratigraphy and argued for the presence of previously undetected hiati in individual sections. Thereby their upward corrected estimate calls for a significantly longer Hettangian, at least 4.1 Myr in duration, which is incompatible with the U-Pb time scale. In contrast, independent astrochronology from the Newark Basin, correlated via magnetostratigraphy with Tethyan marine sections, also suggests a shorter, ~1.7 Myr duration for the Hettangian (Kent et al. 2017). A conservative estimate from the Mochras core in Wales, an exceptional archive of Lower Jurassic stratigraphy, suggests 2.3 ± 0.5 Myr for the Hettangian (Storm et al. 2020).

Astrochronology and other integrated stratigraphic data from Tata

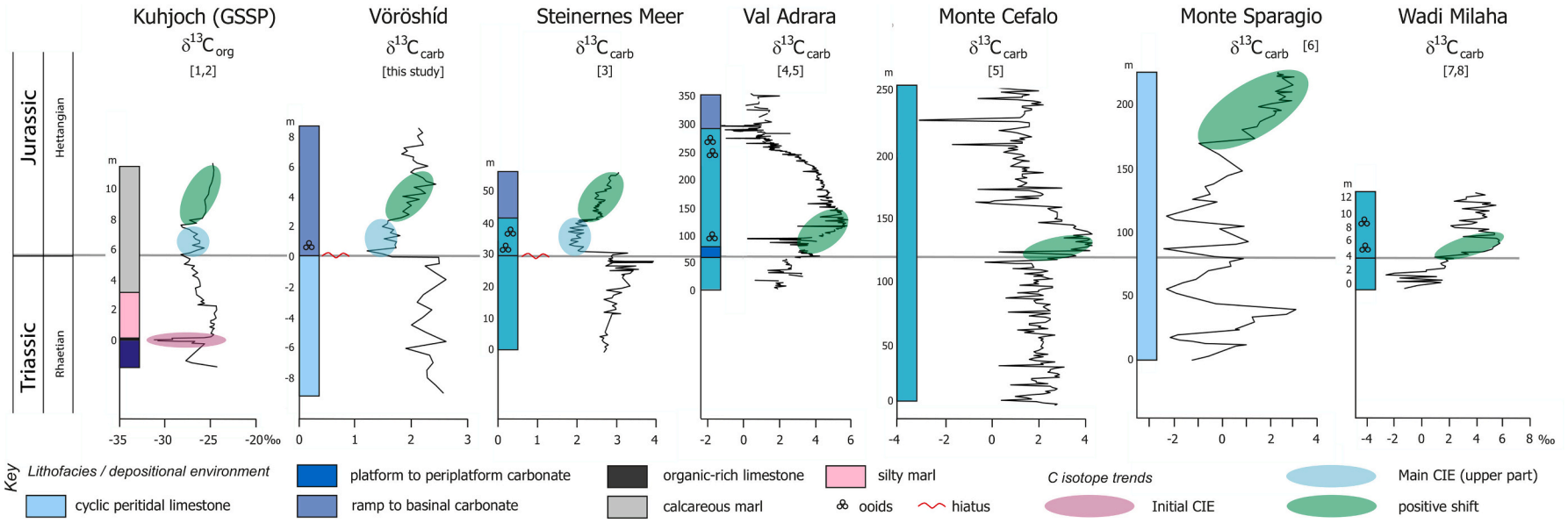

Fig. 15. Carbon isotope stratigraphic correlation of selected shallow marine carbonate successions across the TJB and the GSSP for the base of Jurassic. $\delta^{13}C$ excursions of possible correlation utility are highlighted but note significant differences among sections. Data sources: 1 – Ruhl et al. (2009), 2 – Hillebrandt et al. (2013), 3 – Felber et al. (2015), 4 – van de Schootbrugge et al. (2008), 5 – Bachan et al. (2012), 6 – Todaro et al. (2018), 7 – Al-Suwaidi et al. (2016), 7 – Ge et al. (2018).

suggest that the preserved Hettangian record was deposited in an interval of 1.658–1.947 Myr (with an average of 1.784 Myr). Comparison with the majority view of a Hettangian duration of ~1.8–2.0 Myr therefore supports that the missing Jurassic sedimentary record and hence the length of the gap at the TJB is not more than a few hundreds of thousands of years. This estimate is in agreement with the length of the biostratigraphically missing Lower Hettangian (Ogg and Hinnov 2012). With allowance for an additional ~100 kyr or more between the end-Triassic extinction (marked by the initial CIE that is not preserved at Tata) and the TJB, it still means that the hiatus does not represent an extended period of time.

6.4. Dachstein platform demise and "unreefing" in the context of end-Triassic global change and its effect on shallow marine carbonate systems

A brief review of known or supposed environmental changes at the end-Triassic extinction, and their effect on the carbonate platform systems may help interpret changes in the sedimentary regime around the TJB. Shallow marine platforms represent a sensitive environment and ecosystem that might be vulnerable in times of crises marked by carbon cycle perturbation. Changes in their biological, sedimentological and geochemical properties might be related to changes in atmospheric CO_2 levels that in turn may be involved in complex feedback mechanisms leading to platform drowning (Godet 2013). Independent evidence for sudden and pronounced end-Triassic pCO_2 increase exists from both stomatal density (McElwain et al. 1999, Steinhortsdottir et al., 2011) and isotopic (Schaller et al. 2011) data. Modelling suggests a two-phase response to CO_2 input to the atmosphere-hydrosphere system (Kump et al. 2009). The first phase, 1 to 100 kyr in duration, would lead to ocean acidification, reflected in biocalcification crisis and carbonate dissolution in the seafloor (Greene et al. 2012). Indeed, in a neritic succession in Italy, the change from Zu Fm. to Malanotte Fm. near the TJB represents a drop in carbonate content and concomitant reduction in abundance and size of calcareous nannofossils attributed to the calcification crisis (Galli et al. 2005; Bottini et al. 2016). Similarly, in a somewhat deeper setting of TJB sections in the Eiberg Basin in Austria, lithologic change from limestone of the Kössen Fm. to carbonate-lean terrigenous marl of the Kendelbach Fm. is interpreted as the expression of carbonate productivity decline (Ruhl et al. 2010b). Pelagic carbonate successions in Montenegro also record coeval changes that are interpreted to reflect shoaling of the CCD, the deep water manifestation of the same forcing (Crne et al., 2011). However, the hiatus at the TJB in the studied sections of the Transdanubian Range apparently precluded the preservation of any signal of this phase.

In a second, subsequent phase of longer, million-year duration, the main effect of large scale CO_2 input is the proliferation of chemical carbonate precipitation. Following the decrease of biocalcification, this process can buffer the increase in alkalinity. The Lower Hettangian Lorüns Oolite in the Northern Calcareous Alps records the return of subtidal, periplatform lagoonal carbonate production resulting in the formation of ooidal-oncoidal packstone (McRoberts et al. 1997). Its deposition may also reflect the increasing energy during transgression and higher saturation state after the calcification crisis (Felber et al. 2015). The Albenza Fm. is a widespread time-equivalent deposit in the Southern Alps, recording the resumption of carbonate factory following the carbonate-lean interval of the Malanotte Fm. The lower part is ooidal-oncoidal, containing common microbially coated grains and aggregates and is interpreted as a deposit of calcareous sand bars in a proximal ramp (Jadoul and Galli 2008). This environment replaced platform margin reefs and was stabilized by prolific microbial communities in well-oxygenated shallow water. Both the abundance of ooids and early marine cement may reflect the aftermath of calcification crisis and bloom of cyanobacteria.

In the Transdanubian Range, basal Jurassic layers at Tölgyhát and Vöröshíd are similar in some aspects to the Albenza Fm., albeit with smaller amount of early marine cement and lesser abundance of ooids and oncoids as chemical precipitates. Therefore, direct evidence of ocean acidification is apparently lacking in the studied sections. On the other hand, ooids, oncoids and microbial carbonate components are sufficiently characteristic to infer changes induced by the disappearance of platform margin reefs. A likely scenario is that the end-Triassic environmental crisis resulted in dramatically reduced carbonate production and the extinction of reef builders and reef dwellers. The demise of a rimmed platform, together with a change of bottom water energy regimes facilitated by the earliest Hettangian transgression, resulted in the establishment of a carbonate ramp offshore of a microbially cemented margin of ooidal shoals. This scenario of platform drowning largely driven by the end-Triassic environmental and biotic crisis is consistent with the observed changes in carbonates and is a viable alternative of a tectonically forced subsidence and platform fragmentation. This model explains why an altered and re-established earliest Jurassic carbonate factory could not keep pace with the eustatic sea level change during the Hettangian transgression, whether or not any short-term subaerial exposure occurred at the TJB.

The Dachstein Fm., and Upper Triassic platform carbonates in general, are areally and volumetrically extensive in both the Transdanubian Range and the Northern Calcareous Alps. The studied sections lie in a more poorly exposed but tectonically less complexly deformed region of the once contiguous Neotethyan shelf. Abundant occurrence of *Triasina hantkeni* and other foraminifers (Oravecz-Scheffer 1987) and diverse species of large megalodontid bivalves (Végh-Neubrandt 1982) suggest that platform growth and sedimentation could have continued until the latest Rhaetian. The healthy functioning of the platform and carbonate deposition terminated abruptly. Paleogeographically, the Transdanubian Range preserves a transect of the platform from a reef margin in its northeastern extremity at the Nézsa-Csővár block (Haas et al. 2010) through external lagoons in the east (Gerecse Mts., Tata) to inner platform in the southwest (Bakony Mts.). Paleomagnetic data suggest that present-day orientation reflects 75–90° counter-clockwise rotation during Cenozoic extrusion (Márton and Fodor 2003). As the end-Triassic crisis and global collapse of reef ecosystem removed the rimmed margin, a process termed here as "unreefing", the lagoon lost protection and became exposed to wave erosion. Biotic crisis, exacerbated with ocean acidification, diminished or halted carbonate production, impeded preservation or led to dissolution in shallow environments. Our carbonate petrographic evidence documents the development of resultant shallow marine hardground and hiatus. Paleogeographic polarity of the Transdanubian Range segment of the Dachstein platform explains facies differences between sections in the Gerecse and Bakony Mts. In the Middle Hettangian, under ameliorating conditions, sedimentation in the Gerecse Mts. and Tata resumed on a gradually deepening ramp that replaced the platform, with deposition of the Pisznice Fm. whereas in the Bakony Mts. shallower marine carbonates return (Kardosrét Fm. at Kőris-hegy).

Of the previously proposed models (Fig. 1), major sea-level drop and long-term emergence and subaerial exposure is not compatible with the lack of significant relief and karstification features on the TJB surface and lack of isotopic evidence for pervasive meteoric diagenesis. Platform drowning by tectonically-driven subsidence is not supported by available temporal constraints of main phases of extension. Disintegration by normal faulting is recorded by the Hierlatz Fm., a brachiopodal-crinoidal limestone that accumulated at submarine synsedimentary fault scarps and fissures mostly in the Sinemurian and Pliensbachian (Vörös 1991). Neptunian dykes at Tata and the Gerecse Mts. also postdate the TJB as they originate in Hettangian-Sinemurian strata. Our stable isotope data from pink micritic fissure fills, with $\delta^{13}C$ values of 1.8–2‰, are also compatible with origin in later parts of the Early Jurassic. On the other hand, extensional faulting and formation of intraplatform basins began already in the Late Triassic (Norian-Rhaetian) as demonstrated in the SW part of the Transdanubian Range (Héja et al. 2018). Taken together, we find no support for a short-term extensional event related to the incipient rifting of the Alpine Tethys

that would coincide with the TJB. Instead, the "unreefing" model offers the most parsimonious and likely explanation for the demise of the Dachstein platform in the Transdanubian Range.

These inferences also pertain to the classical area of the Dachstein platform exposed in the Northern Calcareous Alps, where a similar dilemma of subaerial exposure versus submarine non-deposition was also raised with an emphasis on the role of tectonics (Mandl 2000). Deposits of fringing reefs are known from both sides of the platform as *Dachsteinriffkalk* and *Oberrhätkalk*. Although in some places platform drowning is dated to the Early Rhaetian by overlying pelagic deposits (Krystyn et al. 2009), this may be controlled by local extensional tectonics known to take place regionally from the Transdanubian Range to the Southern Alps (Héja et al. 2018). Significant increase in subsidence rates related to the rifting of Alpine Tethys did not start until the Plienbachian (Gawlick et al. 1999). Alternatively, the emergence of the platform was suggested to result from a major end-Triassic sea level drop in excess of 100 m, as inferred from the geometry of *Oberrhätkalk* reefs (Krystyn et al. 2005). However, there is no known evidence of terrestrial karst relief that would be expected to form during an interval of prolonged subaerial exposure under hothouse climate. Instead, the overlying Schnöll Formation rests on an erosional surface that largely inherits reef topography (Böhm et al. 1999). The Langmoos Member of this formation is a close analogue of the Vöröshíd Member of Pisznice Formation that we studied in the Transdanubian Range, both in its lithology, sedimentology and age. The TJB gap is constrained by the occurrence of *Psiloceras naumanni* at the base of the Langmoos Mb., indicating the Early Hettangian Planorbis Zone (Gallet et al. 1993). Here, the sharp contrast and abrupt facies change between the uppermost Rhaetian reef limestone and overlying Lower Hettangian open marine spiculitic biomicrite indicates that the "unreefing" model may provide a suitable explanation of the demise of the entire Dachstein platform.

"Unreefing" fits into a broader context of how ecologically controlled accommodation influences the architecture of carbonate platforms (Pomar 2001; Pomar et al. 2012). The Dachstein platform as a rimmed platform maintained its large extent and profuse carbonate production in the Late Triassic, until the end-Triassic crisis removed the fringing coral reefs from its margins and exposed the inner platform to wave action. Exacerbated by the extinction of much of the other, non-reefal carbonate producing biota, platform growth was abruptly terminated as ecological accommodation was severely reduced. Carbonate sedimentation only resumed after an interval of non-deposition, when a ramp was established below the wave base. The concept of ecological accommodation was developed using Neogene examples of ecologically induced ramp to rimmed platform transition (Pomar 2001, Pomar et al. 2012), whereas in our scenario the opposite is the case when accommodation is lost in the ecological crisis without sea level change playing a major role. During the earliest Hettangian hiatus, the Dachstein platform became a "shaved platform", similar to the Latium-Abruzzi platform in the Appenines, where a Paleogene gap at a paraconformity surface indicates cessation of platform growth and prolonged exposure to submarine wave erosion (Brandano 2017). Shared features include a sharp facies contrast across a flat discontinuity, stylolitic sutures and bioerosion, and a lack of indicators of subaerial exposure.

6.5. The fate of other carbonate platforms at the TJB

Reef gaps, the temporary disappearance of reefs after mass extinctions, are prominent features of the fossil and stratigraphic record (Wood 1999). A Late Triassic acme of reefal biodiversity, area and carbonate production was terminated by the end-Triassic extinction and followed by an Early Jurassic reef gap (Flügel and Kiessling 2002). However, the global Phanerozoic history and productivity of carbonate platforms appear decoupled from that of the reefs, as platforms are generally less affected by biotic extinction (Kiessling et al. 2003). Indeed, many of the carbonate platforms survived elsewhere on the peri-Tethyan shelves into the Early Jurassic despite the reef crisis, including the Dinaric carbonate platform (Crne and Gorican, 2008), the Appenine platform (Mancinelli et al. 2005), the Gavrovo-Tripolitza platform (Pomoni-Papaioannou and Kostopoulou 2008) and the Pelagonian platform (Romano et al. 2008) in the Hellenides, and the Arabian platform in the equatorial Tethys (Ge et al. 2018). Although changes in carbonate production, sedimentology and biota have been recognized in several studies, these carbonate platforms proved resilient during the end-Triassic crisis, despite the global disappearance of platform margin reefs at the end-Triassic extinction. The demise of the Dachstein platform through "unreefing" therefore appears as an exception rather than a rule. This vulnerability may be related to its geographic position as the surviving platforms lied at lower paleolatitude. Further studies need to address if a latitudinal threshold effect, differences in platform geometry, or some other factor may be responsible for differential response to "unreefing". Validity of the model could be verified by finding examples of other reef crises and coincident platform terminations in the global stratigraphic record.

7. Conclusions

An integrated stratigraphic study of several key sections in the Transdanubian Range that capture the TJB at the top of the Dachstein Fm. characterized the hiatal surface and the lowermost Jurassic strata, in order to infer the cause of termination of carbonate platform growth. Whereas most of the previous studies emphasized the role of either emergence and subaerial exposure or tectonically-driven drowning, we demonstrated the key contribution of end-Triassic environmental and biotic changes. The unconformity surface bears signatures of an erosional shallow marine hardground rather than prolonged terrestrial exposure. Stable isotopes mirror sharp facies contrast between prominent peritidal cyclicity in uppermost Triassic strata and lack thereof in the lowermost Jurassic. However, cryptic cyclicity preserved in the distribution of biotic carbonate components allowed astrochronologic duration estimate of ~1.7 Myr for the Hettangian part of the Tata section. Although the length of Hettangian is controversial, the TJB hiatus was likely not longer than a few hundreds of thousands of years. Carbon isotope stratigraphy records an abrupt negative shift at the TJB that suggests that the initial carbon isotope anomaly is not preserved, but overprint by meteoric fluids is also lacking. Taken together, observed changes are best explained by removal of platform margin reefs by the end-Triassic extinction, impeded carbonate production and preservation possibly partly due to acidification, and concomitant drowning and transition from a rimmed platform to carbonate ramp geometry. This model, coined here as "unreefing", appears applicable to the demise of the entire Dachstein platform including its parts in the Northern Calcareous Alps. However, other Late Triassic platforms at more southerly latitudes survived the reef crisis with changes but without drowning.

Declaration of Competing Interest

The authors declare that they have no known competing financial interests or personal relationships that could have appeared to influence the work reported in this paper.

Acknowledgements

We are grateful to István Hegyi and György Czuppon for isotope measurements and help in sample preparation, Birgit Leipner-Mata for assistance in thin section preparation, Géza Császár for providing access to archive thin sections, and Mariann Bosnakoff and Bernát Heszler for technical help. Cyclostratigraphic analyses were initiated by Dávid Bajnai. Discussions with János Haas, Kinga Hips, Michael Joachimski, Axel Munnecke, Orsolya Győri and Andrea Mindszenty helped us greatly in understanding various aspects of carbonates, stratigraphy, and stable

isotopes. Some of the photographs were kindly provided by Orsolya Győri and Zoltán Lantos. Thorough and constructive reviews by Nereo Preto and an anonymous reviewer and comments from guest editor Yadong Sun led to a significantly improved manuscript. Funding from NKFIH OTKA Grant K135309 is acknowledged. The research was partly supported by the European Union and the State of Hungary, co-financed by the European Regional Development Fund in the project of GINOP-2.3.2.-15-2016-00009 'ICER'. This is MTA-MTM-ELTE Paleo contribution No. 333.

Appendix A. Supplementary data

Supplementary data to this article can be found online at https://doi.org/10.1016/j.gloplacha.2021.103428.

References

Allan, J.R., Matthews, R.K., 1982. Isotope signatures associated with early meteoric diagenesis. Sedimentology 29 (6), 797–817.
Al-Suwaidi, A.H., Steuber, T., Suarez, M.B., 2016. The Triassic–Jurassic boundary event from an equatorial carbonate platform (Ghalilah Formation, United Arab Emirates). J. Geol. Soc. 173 (6), 949–953.
Bachan, A., van de Schootbrugge, B., Fiebig, J., McRoberts, C.A., Ciarapica, G., Payne, J. L., 2012. Carbon cycle dynamics following the end-Triassic mass extinction: Constraints from paired δC^{13}_{carb} and δC^{13}_{org} records. Geochem. Geophys. Geosyst. 13, Q09008.
Bernecker, M., 2005. Late Triassic reefs from the Northwest and South Tethys: distribution, setting, and biotic composition. Facies 51 (1–4), 442–453.
Böhm, F., Ebli, O., Krystyn, L., Lobitzer, H., Rakús, M., Siblík, M., 1999. Fauna, stratigraphy and depositional environment of the Hettangian-Sinemurian (Early Jurassic) of Adnet (Salzburg, Österreich). Abhandlungen der geologischen Bundesanstalt 56 (2), 143–271.
Bottini, C., Jadoul, F., Rigo, M., Zaffani, M., Artoni, C., Erba, E., 2016. Calcareous nannofossils at the Triassic/Jurassic boundary: stratigraphic and paleoceanographic characterization. Riv. Ital. Paleontol. Stratigr. 122 (3), 141–164.
Brandano, M., 2017. Unravelling the origin of a Paleogene unconformity in the Latium-Abruzzi carbonate succession: a shaved platform. Palaeogeogr. Palaeoclimatol. Palaeoecol. 485, 687–696.
Budai, T., Fodor, L., Sztanó, O., Kercsmár, Z., Császár, G., Csillag, G., Gál, N., Kele, S., Kiszely, M., Selmeczi, I., Babinszki, E., Thamóné Bozsó, E., Lantos, Z., 2018. A Gerecse hegység földtana. Magyarázó a Gerecse hegység földtani térképéhez (1:50 000). [Geology of the Gerecse Mountains. Explanatory book to the geological map of the Gerecse Mountains (1:50 000)]. Magyarország tájegységi térképsorozata (Regional map series of Hungary). Magyar Bányászati és Földtani Szolgálat Budapest. 490.
Christ, N., Immenhauser, A., Wood, R.A., Darwich, K., Niedermayr, A., 2015. Petrography and environmental controls on the formation of Phanerozoic marine carbonate hardgrounds. Earth Sci. Rev. 151, 176–226.
Črne, A.E., Goričan, S., 2008. The Dinaric Carbonate Platform margin in the Early Jurassic: a comparison between successions in Slovenia and Montenegro. Bolletino della Societŕ Geolologica Italiana 127, 389–405.
Črne, A.E., Weissert, H., Goričan, S., Bernasconi, S.M., 2011. A biocalcification crisis at the Triassic-Jurassic boundary recorded in the Budva Basin (Dinarides, Montenegro). Geol. Soc. Am. Bull. 123 (1–2), 40–50.
Császár, G., Oravecz-Scheffer, A., 1987. Bakony, Bakonybél, Kőris-hegy. In: Magyarország geológiai alapszelvényei (Geological Reference Sections of Hungary). Magyar Állami Földtani Intézet (Hungarian Geological Institute), Budapest, p. 6.
Császár, G., Galácz, A., Vörös, A., 1998. A gerecsei jura – fácieskérdések, alpi analógiák (Jurassic of the Gerecse Mountains, Hungary: facies and Alpine analogies). Földtani Közlöny (Bulletin of the Hungarian Geological Society) 128 (2–3), 397–435.
Csontos, L., Vörös, A., 2004. Mesozoic plate tectonic reconstruction of the Carpathian region. Palaeogeogr. Palaeoclimatol. Palaeoecol. 210 (1), 1–56.
Dulai, A., 1998. Early Jurassic brachiopods from the basal layers of the Pisznice Limestone of Lábatlan (Gerecse Mts, Hungary). Annales Historico-Naturales Musei Nationalis Hungarici 90, 35–55.
Dunham, R.J., 1962. Classification of carbonate rocks according to depositional texture. AAPG Mem. 1, 108–121.
Enos, P., Samankassou, E., 1998. Lofer cyclothems revisited (late Triassic, northern Alps, Austria). Facies 38 (1), 207–227.
Felber, R., Weissert, H.J., Furrer, H., Bontognali, T.R.R., 2015. The Triassic–Jurassic boundary in the shallow-water marine carbonates from the western Northern Calcareous Alps (Austria). Swiss J. Geosci. 1–12.
Fischer, A.G., 1964. The Lofer cyclothems of the Alpine Triassic. Kansas Geological Survey Bulletin 169, 107–149.
Flügel, E., Kiessling, W., 2002. Patterns of Phanerozoic reef crises. In: Kiessling, W., Flügel, E., Golonka, J. (Eds.), Phanerozoic Reef Patterns. SEPM (Society for Sedimentary Geology), Tulsa, Oklahoma, pp. 691–733.
Flügel, E., Munnecke, A., 2010. Microfacies of Carbonate Rocks: Analysis, Interpretation and Application. Springer, Berlin, p. 984.
Fülöp, J., 1976. Tatai mezozóos alaphegység-rögök (The Mesozoic basement horst blocks of Tata). Geologica Hungarica, Series Geologica 16, 1–228.
Gallet, Y., Vandamme, D., Krystyn, L., 1993. Magnetostratigraphy of the Hettangian Langmoos Section (Adnet, Austria) - evidence for Time-Delayed Phases of Magnetization. Geophys. J. Int. 115 (2), 575–585.
Galli, M.T., Jadoul, F., Bernasconi, S.M., Weissert, H., 2005. Anomalies in global carbon cycling and extinction at the Triassic/Jurassic boundary: evidence from a marine C-isotope record. Palaeogeogr. Palaeoclimatol. Palaeoecol. 216 (3–4), 203–214.
Gawlick, H.-J., Frisch, W., Vecsei, A., Steiger, T., Böhm, F., 1999. The change from rifting to thrusting in the Northern Calcareous Alps as recorded in Jurassic sediments. Geol. Rundsch. 87 (4), 644–657.
Gawlick, H.-J., Missoni, S., Schlagintweit, F., Suzuki, H., Frisch, W., Krystyn, L., Blau, J., Lein, R., 2009. Jurassic tectonostratigraphy of the Austroalpine domain. J. Alpine Geol. 50, 1–152.
Ge, Y., Shi, M., Steuber, T., Al-Suwaidi, A.H., Suarez, M.B., 2018. Environmental change during the Triassic–Jurassic boundary interval of an equatorial carbonate platform: Sedimentology and chemostratigraphy of the Ghalilah Formation, United Arab Emirates. Palaeogeogr. Palaeoclimatol. Palaeoecol. 502, 86–103.
Godet, A., 2013. Drowning unconformities: Palaeoenvironmental significance and involvement of global processes. Sediment. Geol. 293, 45–66.
Greene, S.E., Martindale, R.C., Ritterbush, K.A., Bottjer, D.J., Corsetti, F.A., Berelson, W. M., 2012. Recognising Ocean acidification in deep time: an evaluation of the evidence for acidification across the Triassic-Jurassic boundary. Earth Sci. Rev. 113 (1–2), 72–93.
Guex, J., Schoene, B., Bartolini, A., Spangenberg, J., Schaltegger, U., O'Dogherty, L., Taylor, D., Bucher, H., Atudorei, V., 2012. Geochronological constraints on post-extinction recovery of the ammonoids and carbon cycle perturbations during the Early Jurassic. Palaeogeogr. Palaeoclimatol. Palaeoecol. 346, 1–11.
Győri, O., 2014. Paleofluidum-áramlási események nyomozása dunántúli-középhegységi mezozoos karbonátokban. Eötvös Loránd Tudományegyetem, Budapest, 147+xxi pp.
Haas, J., 1994. Lofer Cycles of the Upper Triassic Dachstein Platform in the Transdanubian Mid-Mountains (Hungary). In: de Boer, P.L., Smith, D.G. (Eds.), Orbital Forcing and Cyclic Sequences. Spec. Publs Int. Ass. Sediment, pp. 303–322.
Haas, J., 1995a. Az Északi Gerecse felsőtriász karbonát platform képződményei (Upper Triassic platform carbonates in the Northern Gerecse Mts.). Földtani Közlöny (Bulletin of the Hungarian Geological Society) 125, 259–293.
Haas, J., 1995b. Upper Triassic platform carbonates in the Northern Bakony Mts. Földtani Közlöny (Bulletin of the Hungarian Geological Society) 125, 27–64.
Haas, J., 2002. Origin and evolution of Late Triassic platform carbonates in the Transdanubian Range (Hungary). Geol. Carpath. 53, 159–178.
Haas, J., 2004. Characteristics of peritidal facies and evidences for subaerial exposures in Dachstein-type cyclic platform carbonates in the Transdanubian Range, Hungary. Facies 50 (2), 263–286.
Haas, J., Budai, T., 2014. Stratigraphic and facies problems of the Upper Triassic in the Transdanubian Range: reconsideration of old problems on the basis of new results. Földtani Közlöny 144 (2), 125–142.
Haas, J., Hámor, G., 2001. Geological garden in the neighborhood of Budapest, Hungary. Episodes 24 (4), 257–261.
Haas, J., Kovács, S., Krystyn, L., Lein, R., 1995. Significance of late Permian - Triassic facies zones in terrane reconstructions in the Alpine North Pannonian domain. Tectonophysics 242 (1), 19–40.
Haas, J., Lobitzer, H., Monostori, M., 2007. Characteristics of the Lofer cyclicity in the type locality of the Dachstein Limestone (Dachstein Plateau, Austria). Facies 53 (1), 113–126.
Haas, J., Götz, A.E., Pálfy, J., 2010. Late Triassic to Early Jurassic palaeogeography and eustatic history in the NW Tethyan realm: New insights from sedimentary and organic facies of the Csovar Basin (Hungary). Palaeogeogr. Palaeoclimatol. Palaeoecol. 291 (3–4), 456–468.
Haas, J., Kovács, S., Gawlick, H.-J., Grădinaru, E., Karamata, S., Sudar, M., Péró, C., Mello, J., Polák, M., Ogorelec, B., Buser, S., 2011. Jurassic Evolution of the Tectonostratigraphic units of the Circum-Pannonian Region. Jahrb. Geol. Bundesanst. 151 (3–4), 281–354.
Haas, J., Győri, O., Kocsis, Á.T., Lantos, Z., Pálfy, J., 2018. A triász és a jura időszak határán lezajlott globális krízis és annak nyomai magyarországi rétegsorokban. Földtani Közlöny 148 (1), 9–26.
Hautmann, M., 2004. Effect of end-Triassic CO2 maximum on carbonate sedimentation and marine mass extinction. Facies 50, 257–261.
Héja, G., Kövér, S., Csillag, G., Németh, A., Fodor, L., 2018. Evidences for pre-orogenic passive-margin extension in a Cretaceous fold-and-thrust belt on the basis of combined seismic and field data (western Transdanubian Range, Hungary). Int. J. Earth Sci. 107, 2955–2973.
Hesselbo, S.P., Robinson, S.A., Surlyk, F., Piasecki, S., 2002. Terrestrial and marine mass extinction at the Triassic–Jurassic boundary synchronized with major carbon-cycle perturbation: a link to initiation of massive volcanism? Geology 30 (3), 251–254.
Hillebrandt, A.v., Krystyn, L., Kürschner, W.M., Bonis, N.R., Ruhl, M., Richoz, S., Schobben, M.A.N., Urlichs, M., Bown, P.R., Kment, K., McRoberts, C.A., Simms, M., Tomásových, A., 2013. The Global Stratotype Sections and Point (GSSP) for the base of the Jurassic System at Kuhjoch (Karwendel Mountains, Northern Calcareous Alps, Tyrol, Austria). Episodes 36 (3), 162–198.
Hillgärtner, H., 1998. Discontinuity surfaces on a shallow-marine carbonate platform (Berriasian, Valanginian, France and Switzerland). J. Sediment. Res. 68 (6), 1093–1108.
Hinnov, L., Hilgen, F., 2012. Cyclostratigraphy and astrochronology. In: Gradstein, F.M., Ogg, J.G., Schmitz, M.D., Ogg, G. (Eds.), The Geologic Time Scale 2012. Elsevier, Amsterdam, pp. 63–83.
Hüsing, S.K., Beniest, A., van der Boon, A., Abels, H.A., Deenen, M.H.L., Ruhl, M., Krijgsman, W., 2014. Astronomically-calibrated magnetostratigraphy of the lower Jurassic marine successions at St. Audrie's Bay and East Quantoxhead

(Hettangian–Sinemurian; Somerset, UK). Palaeogeogr. Palaeoclimatol. Palaeoecol. 403, 43–56.
Jadoul, F., Galli, M.T., 2008. The Hettangian shallow water carbonates after the Triassic/Jukassic biocalcification crisis: the Albenza Formation in the western Southern Alps. Riv. Ital. Paleontol. Stratigr. 114 (3), 453–470.
Joachimski, M.M., 1994. Subaerial exposure and deposition of shallowing upward sequences: evidence from stable isotopes of Purbeckian peritidal carbonates (basal Cretaceous), Swiss and French Jura Mountains. Sedimentology 41 (4), 805–824.
Kent, D.V., Olsen, P.E., Muttoni, G., 2017. Astrochronostratigraphic Polarity Time Scale (APTS) for the Late Triassic and Early Jurassic from Continental Sediments and Correlation with Standard Marine Stages. Earth Sci. Rev. 166, 153–180.
Kiessling, W., Flügel, E., Golonka, J.A.N., 2003. Patterns of Phanerozoic carbonate platform sedimentation. Lethaia 36 (3), 195–225.
Kiessling, W., Aberhan, M., Brenneis, B., Wagner, P.J., 2007. Extinction trajectories of benthic organisms across the Triassic-Jurassic boundary. Palaeogeogr. Palaeoclimatol. Palaeoecol. 224, 201–222.
Koch, N., 1909. A tatai Kálváriadomb földtani viszonyai. Földtani Közlöny 39 (5), 255–275.
Konda, J., 1985. Gerecse, Lábatlan, Nagypisznicei kőfejtő (Gerecse, Lábatlan, Nagypisznice quarry). Magyarország geológiai alapszelvényei. Magyar Állami Földtani Intézet (Hungarian Geological Institute), p. 10.
Konda, J., 1987. Gerecse, Süttő, Vöröshídi-kőfejtő (Gerecse, Süttő, Vöröshíd quarry). Magyarország geológiai alapszelvényei. Magyar Állami Földtani Intézet (Hungarian Geological Institute), p. 10.
Konda, J., 1988. Gerecse, Lábatlan, Tölgyháti kőfejtő (Gerecse, Lábatlan, Tölgyhát quarry). In: Magyarország geológiai alapszelvényei [Geological Reference Sections of Hungary]. Állami Földtani Intézet (Hungarian Geological Institute), Magyar, p. 8.
Korte, C., Ruhl, M., Pálfy, J., Ullmann, C.V., Hesselbo, S.P., 2019. Chemostratigraphy across the Triassic–Jurassic boundary. In: Sial, A.N., Gaucher, C., Ramkumar, M., Ferreira, V.P. (Eds.), Chemostratigraphy Across Major Chronological Boundaries. AGU Geophysical Monograph Series, pp. 185–210.
Krystyn, L., Böhm, F., Kürschner, W., Delecat, S., 2005. The Triassic–Jurassic boundary in the Northern Calcareous Alps. In: Pálfy, J., Ozsvárt, P. (Eds.), Program, Abstracts and Field Guide. 5th Field Workshop of IGCP 458 Project (Tata and Hallein). A1-A14.
Krystyn, L., Mandl, G.W., Schauer, M., 2009. Growth and termination of the Upper Triassic platform margin of the Dachstein area (Northern Calcareous Alps, Austria). Austrian J. Earth Sci. 102 (1), 23–33.
Kump, L.R., Bralower, T.J., Ridgwell, A., 2009. Ocean acidification in deep time. Oceanography 22 (4), 94–107.
Landis, G.P., 1983. Harding Iceland spar: a new $\delta^{18}O-\delta^{13}C$ carbonate standard for hydrothermal minerals. Chem. Geol. 41, 91–94.
Lantos, Z., 1997. Karbonátos lejtő-üledékképződés egy liász tengeralatti magaslat oldalában, eltolódásos vetőzóna mentén (Gerecse). Földtani Közlöny 127 (3–4), 291–312.
Laskar, J., Robutel, P., Joutel, F., Gastineau, M., Correia, A.C.M., Levrard, B., 2004. A long-term numerical solution for the insolation quantities of the Earth. Astronomy Astrophysics 428 (1), 261–285.
Li, M., Hinnov, L., Kump, L., 2019. Acycle: Time-series analysis software for paleoclimate research and education. Comput. Geosci. 127, 12–22.
Mancinelli, A., Chiocchini, M., Chiocchini, R.A., Romano, A., 2005. Biostratigraphy of Upper Triassic-Lower Jurassic carbonate platform sediments of the central-southern Apennines (Italy). Riv. Ital. Paleontol. Stratigr. 111 (2), 271–283.
Mandl, G.W., 2000. The Alpine sector of Tethyan shelf – examples of Triassic to Jurassic sedimentation and deformation from the Northern Calcareous Alps. Mitteilungen der Österreichischen Geologischen Gesellschaft 92, 61–77.
Marshall, J.D., 1992. Climatic and oceanographic isotopic signals from the carbonate rock record and their preservation. Geol. Mag. 129 (2), 143–160.
Martindale, R.C., Krystyn, L., Corsetti, F.A., Bottjer, D.J., 2013. From fore reef to lagoon: Evolution of the Upper Triassic Dachstein carbonate platform on the Tennengebirge (Salzburg, Austria). Palaios 28 (11), 755–770.
Márton, E., Fodor, L., 2003. Tertiary paleomagnetic results and structural analysis from the Transdanubian Range (Hungary): rotational disintegration of the Alcapa unit. Tectonophysics 363 (3–4), 201–224.
Márton, E., Márton, P., 1981. Mesozoic palaeomagnetism of the Transdanubian Central Mountains and its tectonic implications. Tectonophysics 72 (1–2), 129–140.
McElwain, J.C., Beerling, D.J., Woodward, F.I., 1999. Fossil plants and global warming at the Triassic-Jurassic Boundary. Science 285 (5432), 1386–1390.
McRoberts, C.A., Furrer, H., Jones, D.S., 1997. Palaeoenvironmental interpretation of a Triassic-Jurassic boundary section from Western Austria based on palaeoecological and geochemical data. Palaeogeogr. Palaeoclimatol. Palaeoecol. 136, 79–95.
Mette, W., Elsler, A., Korte, C., 2012. Palaeoenvironmental changes in the Late Triassic (Rhaetian) of the Northern Calcareous Alps: Clues from stable isotopes and microfossils. Palaeogeogr. Palaeoclimatol. Palaeoecol. 350-352, 62–72.
Missoni, S., Gawlick, H.-J., 2011. Evidence for Jurassic subduction from the Northern Calcareous Alps (Berchtesgaden; Austroalpine, Germany). Int. J. Earth Sci. 100 (7), 1605–1631.
Ogg, J.G., Hinnov, L.A., 2012. Jurassic. In: Gradstein, F.M., Ogg, J.G., Schmitz, M.D., Ogg, G. (Eds.), The Geologic Time Scale 2012. Elsevier, pp. 731–791.
Ogg, J.G., Ogg, G.M., Gradstein, F.M., 2016. A Concise Geologic Time Scale 2016. Elsevier, Amsterdam, p. 240.
Oravecz-Scheffer, A., 1987. Triassic foraminifers of the Transdanubian Central Range. Geologica Hungarica, Series Palaeontologica 50, 1–331.
Pálfy, J., Kocsis, T.Á., 2014. Volcanism of the Central Atlantic Magmatic Province as the trigger of environmental and biotic changes around the Triassic-Jurassic boundary. In: Keller, G., Kerr, A.C. (Eds.), Volcanism, Impacts and Mass Extinctions: Causes and Effects. Geological Society of America Special Paper. Geological Society of America, Boulder, CO, pp. 245–261.
Pálfy, J., Demény, A., Haas, J., Hetényi, M., Orchard, M., Vető, I., 2001. Carbon isotope anomaly and other geochemical changes at the Triassic-Jurassic boundary from a marine section in Hungary. Geology 29 (11), 1047–1050.
Pálfy, J., Dulai, A., Szente, I., 2007. Kálvária-dombi kőfejtő nyugati udvara. In: Pálfy, J., Pazonyi, P. (Eds.), Őslénytani kirándulások Magyarországon és Erdélyben. Hantken Kiadó, Budapest, pp. 41–44.
Pomar, L., 2001. Ecological control of sedimentary accommodation: evolution from a carbonate ramp to rimmed shelf, Upper Miocene, Balearic Islands. Palaeogeogr. Palaeoclimatol. Palaeoecol. 175 (1), 249–272.
Pomar, L., Bassant, P., Brandano, M., Ruchonnet, C., Janson, X., 2012. Impact of carbonate producing biota on platform architecture: Insights from Miocene examples of the Mediterranean region. Earth Sci. Rev. 113, 186–211.
Pomoni-Papaioannou, F., Kostopoulou, V., 2008. Microfacies and cycle stacking pattern in Liassic peritidal carbonate platform strata, Gavrovo-Tripolitza platform, Peloponnesus, Greece. Facies 54 (3), 417–431.
Rameil, N., Immenhauser, A., Csoma, A.É., Warrlich, G., 2012. Surfaces with a long history: the Aptian top Shu'aiba Formation unconformity, Sultanate of Oman. Sedimentology 59 (1), 212–248.
Ratschbacher, L., Frisch, W., Linzer, H.-G., Merle, O., 1991. Lateral extrusion in the Eastern Alps, Part 2: Structural analysis. Tectonics 10, 257–271.
Romano, R., Masett, D., Carras, N., Barattolo, F., Roghi, G., 2008. The Triassic/Jurassic boundary in a peritidal carbonate platform of the Pelagonian domain: the Mount Messapion section (Chalkida, Greece). Riv. Ital. Paleontol. Stratigr. 114 (3), 431–452.
Ruhl, M., Kuerschner, W.M., Krystyn, L., 2009. Triassic-Jurassic organic carbon isotope stratigraphy of key sections in the western Tethys realm (Austria). Earth Planet. Sci. Lett. 281 (3–4), 169–187.
Ruhl, M., Deenen, M.H.L., Abels, H.A., Bonis, N.R., Krijgsman, W., Kürschner, W.M., 2010a. Astronomical constraints on the duration of the early Jurassic Hettangian stage and recovery rates following the end-Triassic mass extinction (St Audrie's Bay/East Quantoxhead, UK). Earth Planet. Sci. Lett. 295 (1–2), 262–276.
Ruhl, M., Veld, H., Kürschner, W.M., 2010b. Sedimentary organic matter characterization of the Triassic-Jurassic boundary GSSP at Kuhjoch (Austria). Earth Planet. Sci. Lett. 292 (1–2), 17–26.
Schaller, M.F., Wright, J.D., Kent, D.V., 2011. Atmospheric pCO2 perturbations associated with the Central Atlantic Magmatic Province. Science 331 (6023), 1404–1409.
Schaltegger, U., Guex, J., Bartolini, A., Schoene, B., Ovtcharova, M., 2008. Precise U-Pb age constraints for end-Triassic mass extinction, its correlation to volcanism and Hettangian post-extinction recovery. Earth Planet. Sci. Lett. 267 (1–2), 266–275.
Schoene, B., Guex, J., Bartolini, A., Schaltegger, U., Blackburn, T.J., 2010. Correlating the end-Triassic mass extinction and flood basalt volcanism at the 100 ka level. Geology 38 (5), 387–390.
Spötl, C., Vennemann, T.W., 2003. Continuous-flow isotope ratio mass spectrometric analysis of carbonate minerals. Rapid Commun. Mass Spectrom. 17 (9), 1004–1006.
Steinthorsdottir, M., Jeram, A.J., McElwain, J.C., 2011. Extremely elevated CO2 concentrations at the Triassic/Jurassic boundary. Palaeogeogr. Palaeoclimatol. Palaeoecol. 308 (3–4), 418–432.
Storm, M.S., Hesselbo, S.P., Jenkyns, H.C., Ruhl, M., Ullmann, C.V., Xu, W., Leng, M.J., Riding, J.B., Gorbanenko, O., 2020. Orbital pacing and secular evolution of the Early Jurassic carbon cycle. Proc. Natl. Acad. Sci. 117 (8), 3974–3982.
Tari, G., Horváth, F., 2010. A Dunántúli-középhegység helyzete és eoalpi fejlődéstörténete a Keleti-Alpok takarós rendszerében: egy másfél évtizedes tektonikai modell időszerűsége (Eo-alpine evolution of the transdanubian range in the nappe system of the Eastern Alps: Revival of a 15 years old tectonic model). Foldtani Kozlony 140 (4), 483–510.
Thomson, D.J., 1982. Spectrum estimation and harmonic analysis. Proc. IEEE 70 (9), 1055–1096.
Thomson, D.J., 1990. Quadratic-inverse spectrum estimates: applications to palaeoclimatology. Phil. Trans. R. Soc. A 332, 539–597.
Todaro, S., Rigo, M., Randazzo, V., Di Stefano, P., 2018. The end-Triassic mass extinction: a new correlation between extinction events and $\delta^{13}C$ fluctuations from a Triassic-Jurassic peritidal succession in western Sicily. Sediment. Geol. 368, 105–113.
van de Schootbrugge, B., Payne, J.L., Tomasovych, A., Pross, J., Fiebig, J., Benbrahim, M., Follmi, K.B., Quan, T.M., 2008. Carbon cycle perturbation and stabilization in the wake of the Triassic-Jurassic boundary mass-extinction event. Geochemistry Geophysics Geosystems 9 (4), 1–16.
Szabó, I., 1961. A tatai mezozóos rög júra kifejlődései. Magyar Állami Földtani Intézet Évkönyve 49 (2), 469–474.
Végh-Neubrandt, E., 1982. Triassische Megalodontaceae. In: Entwicklung, Stratigraphie und Paläontologie. Budapest, Akadémiai Kiadó, p. 526.
Vigh, G., 1936. Rétegtani és hegyszerkezeti megfigyelések a Nagypisznice környékén. A Magyar Kir. Földtani Intézet évi jelentése(1933-1935 IV), pp. 1455–1466.
Vigh, G., 1961a. A Gerecse-hegység nyugati felének földtani vázlata. A Magyar Állami Földtani Intézet Évkönyve 49 (2), 445–462.
Vigh, G., 1961b. A gerecsei júra üledékek fácieskérdései. A Magyar Állami Földtani Intézet Évkönyve 49 (2), 463–468.
Vörös, A., 1991. Hierlatzkalk – A peculiar Austro-Hungarian Jurassic facies. In: Lobitzer, H., Császár, G. (Eds.), Jubiläumsschrift 20 Jahre Geologische Zusammenarbeit Österreich–Ungarn, pp. 145–154. Teil 1.
Vörös, A., Galácz, A., 1998. Jurassic palaeogeography of the Transdanubian Central Range (Hungary). Riv. Ital. Paleontol. Stratigr. 104 (1), 69–84.

Ward, P.D., Haggart, J.W., Carter, E.S., Wilbur, D., Tipper, H.W., Evans, T., 2001. Sudden productivity collapse associated with the Triassic-Jurassic boundary mass extinction. Science 292, 1148–1151.
Weedon, G.P., Page, K.N., Jenkyns, H.C., 2019. Cyclostratigraphy, stratigraphic gaps and the duration of the Hettangian Stage (Jurassic): insights from the Blue Lias Formation of southern Britain. Geol. Mag. 156 (9), 1469–1509.
Wood, R., 1999. Reef Evolution. Oxford University Press, Oxford, p. 426.
Wotzlaw, J.-F., Guex, J., Bartolini, A., Gallet, Y., Krystyn, L., McRoberts, C.A., Taylor, D., Schoene, B., Schaltegger, U., 2014. Towards accurate numerical calibration of the Late Triassic: High-precision U-Pb geochronology constraints on the duration of the Rhaetian. Geology 42, 571–574.